UNCLASSIFIED

C.1

NACA RM E56J17

RESEARCH MEMORANDUM

EXPERIMENTAL INVESTIGATION OF AN AXIAL-FLOW-COMPRESSOR INLET STAGE OPERATING AT TRANSONIC RELATIVE INLET MACH NUMBERS

V - ROTOR BLADE-ELEMENT PERFORMANCE AT A REDUCED BLADE ANGLE

By Francis C. Schwenk, George W. Lewis, Jr., and Seymour Lieblein

Lewis Flight Propulsion Laboratory
Cleveland, Ohio

CLASSIFICATION CHANGED
To UNCLASSIFIED
By authority of Rese RA 2 Date 12-31-58
NB 1-30-59

LIBRARY COPY
FEB 1 1957
LANGLEY AERONAUTICAL LABORATORY
LIBRARY NACA
LANGLEY FIELD, VIRGINIA

CLASSIFIED DOCUMENT

This material contains information affecting the National Defense of the United States within the meaning of the espionage laws, Title 18, U.S.C., Secs. 793 and 794, the transmission or revelation of which in any manner to an unauthorized person is prohibited by law.

NATIONAL ADVISORY COMMITTEE FOR AERONAUTICS

WASHINGTON

January 24, 1957

CONFIDENTIAL

UNCLASSIFIED

NASA Technical Library
3 1176 01436 0912

NACA RM E56J17

NATIONAL ADVISORY COMMITTEE FOR AERONAUTICS

RESEARCH MEMORANDUM

EXPERIMENTAL INVESTIGATION OF AN AXIAL-FLOW-COMPRESSOR INLET STAGE OPERATING AT TRANSONIC RELATIVE INLET MACH NUMBERS

V - ROTOR BLADE-ELEMENT PERFORMANCE AT A REDUCED BLADE ANGLE

By Francis C. Schwenk, George W. Lewis, Jr., and Seymour Lieblein

3888

CN-1

SUMMARY

A transonic axial-flow-compressor rotor was tested with low blade angles. The rotor contained the blades used in a previous investigation, but they were set in a new rotor disk at a setting angle 6° closer to the axial direction than in the original rotor. Over-all and blade-element performance of the low-blade-angle rotor are given herein. The performance is compared with the original rotor and other transonic-compressor rotor data.

At a corrected speed of 1100 feet per second, the low-blade-angle rotor operated with a relative inlet Mach number of 1.2, a diffusion factor of 0.65, and an axial velocity ratio of 0.71 in the tip region (11 percent of the passage height away from the outer wall). The measured minimum loss coefficient was 0.35, which value falls above a previous correlation of rotor losses with diffusion factor. Through a comparison with data for three other rotors, the occurrence of high losses was related to a high suction-surface Mach number. These comparisons also indicated that axial velocity ratios between 0.73 and 1.10 have no independent effect on losses.

INTRODUCTION

Current design procedures for transonic axial-flow compressors use blade-element data or cascade data in the selection of blades, and it is necessary that these data be available for a wide range of design conditions (relative Mach number level, loading, solidity, blade angle, camber angle, etc.). Therefore, the transonic-compressor rotor discussed in this report was tested to provide some blade-element data for conditions somewhat different from those associated with previously reported rotor data.

C[redacted]

The rotor was constructed by placing the blades used in the compressor of references 1 to 4 in a new rotor disk at a blade angle 6° below the original value; therefore, all the blade angles are 6° lower than angles of the original rotor. The reduction in blade-setting angle should produce, at a given rotational speed, higher inlet relative Mach numbers (near 1.2) than were observed in tests of the original rotor (refs. 1, 3, and 4). Tip-section camber angles of 22.1° also made the tests of the rotor interesting, since most of the transonic-compressor rotors for which data are available have lower tip-section camber (refs. 5 to 9).

3888

The rotor with the low blade angle was tested over a range of weight flows at corrected tip speeds of 600, 800, 900, 1000, and 1100 feet per second. From detailed measurements, blade-element data were computed and are presented in this report. The blade-element losses of several other transonic-compressor rotors are compared with the low-blade-angle rotor data to study the flow characteristics that may influence compressor losses.

Over-all performance and rotor-inlet and -outlet conditions for the low-blade-angle rotor are also presented.

SYMBOLS

A_F compressor frontal area based on rotor tip diameter, sq ft

a speed of sound, ft/sec

b height of stream tube

c_p specific heat of air at constant pressure, Btu/(lb)($^{\circ}$R)

D diffusion factor, $1 - \frac{V_4'}{V_3'} + \frac{\Delta V_\theta}{2\sigma V_3'}$

g acceleration due to gravity, 32.17 ft/sec^2

H total enthalpy, $c_p g J T$, sq ft/sec^2

i incidence angle, angle between inlet relative air-velocity vector and tangent to blade mean camber line at leading edge, deg

J mechanical equivalent of heat, 778 ft-lb/Btu

M Mach number

[redacted]

3888

CW-1 back

P	total pressure, lb/sq ft
r	radius measured from axis of rotation, in.
T	absolute total temperature, $^{\circ}R$
U	blade speed, ft/sec
V	air velocity, ft/sec
w	air weight flow, lb/sec
x	percent of passage height
β	air angle, angle between air velocity and axial direction, deg
δ	ratio of inlet total pressure to NACA standard sea-level total pressure of 2116.22 lb/sq ft
δ°	deviation angle, angle between outlet relative air-velocity vector and tangent to blade mean camber line at trailing edge, deg
η	adiabatic temperature-rise efficiency
θ	ratio of inlet total temperature to NACA standard sea-level temperature of 518.688° R
$\varkappa$	blade angle, angle between tangent to blade mean camber line at leading or trailing edge and axial direction, deg
ρ	static density of air, lb/cu ft
σ	solidity, ratio of blade chord measured along streamline to average blade spacing
$\bar{\omega}$	total-pressure-loss coefficient

Subscripts:

a	stagnation conditions
b	blade element
C	compressor
h	hub
m	mean radius

[redacted]

s suction surface

t tip

th throat

z axial direction

θ tangential direction

1 depression tank

2 weight-flow measuring station upstream of rotor

2-D two-dimensional cascade

3 rotor inlet

4 rotor outlet

Superscript:

' relative to rotor

3888

APPARATUS AND PROCEDURE

Compressor Rotor

The 21 rotor blades employed in the compressors described in references 1 to 4 were installed in a rotor disk at a slot angle 6° closer to the rotor axis than in the original compressor. For comparison purposes, blade angles for the original rotor and for the low-blade-angle rotor are shown in table I for four blade sections. Solidities are also given. Reference 2 presents design blade coordinates for these rotor blades. The tip section is approximately a double-circular-arc airfoil; however, the hub section differs from a double-circular-arc airfoil in that the maximum thickness and the maximum camber are located at the 60-percent-chord point.

Instrumentation and Procedure

The low-blade-angle rotor was tested without inlet guide vanes or discharge stators in the same research facility employed in the investigations reported in references 1, 3, and 4. A schematic diagram of the compressor test section showing the instrument locations is given in figure 1. Instrumentation is described in detail in reference 3.

Weight flow was determined from a calibrated orifice in the inlet piping system. Rotor-entrance flow characteristics were obtained from wall static taps, a fixed static rake, and inlet tank temperatures and pressures.

Rotor outlet (station 4, about 1/2 in. downstream) conditions were obtained from radial surveys of total pressure, static pressure, and flow angle, fixed radial thermocouple rakes, and static taps on the inner and outer walls.

3888

Area-averaged over-all performance of the rotor was determined from fixed Kiel-type radial total-pressure probes, total-temperature rakes, and inner- and outer-wall static taps at station 6 approximately 6 inches downstream of the rotor.

For these tests, the compressor rotor was operated at five corrected tip speeds: 600, 800, 900, 1000, and 1100 feet per second. For tip speeds up to 1000 feet per second, ambient inlet conditions were used. However, to avoid centrifugal-stress problems at 1100 feet per second, refrigerated air was mixed with ambient air, resulting in inlet temperatures of from 32° to 38° F.

Calculation procedures are described in reference 3. The radial survey data measured at station 4 provided the basis for calculating the rotor blade-element and mass-averaged performance characteristics. The mass-averaged performance was compared with and supplemented by the area-averaged results determined from the measurements made at station 6.

It is almost impossible to assign values for the accuracy of a specific measurement in a compressor test, mainly because of the unsteady flow and interference effects on the measuring probes. A certain amount of redundancy occurs in the taking of data, and this factor makes possible certain comparisons that indicate the quality of the data. Weight flows integrated from measurements made at both stations 2 and 4 differ only 1.5 percent from the weight flows indicated by the orifice for all operating conditions except those at low flow rates at low speeds. Mass-averaged adiabatic efficiencies based on temperature rise and tangential momentum agreed within about 3 percent. A similar agreement existed between the mass-averaged temperature-rise efficiency at station 4 and the efficiency computed from the data recorded at station 6. Thus, it appears that generally consistent data were recorded in the tests of the low-blade-angle rotor.

[redacted]

PERFORMANCE OF LOW-BLADE-ANGLE ROTOR

Over-All Performance

The over-all total-pressure ratio and the adiabatic temperature-rise efficiency for the low-blade-angle rotor are plotted against corrected weight flow per unit of frontal area (specific weight flow) in figure 2. Data for corrected tip speeds of 600, 800, 900, 1000, and 1100 feet per second are given. Most of the results represent the mass-averaged performance; however, the flagged symbols indicate pressure ratios and efficiencies determined from area-averaging the data taken with fixed probes at station 6. For these operating conditions, no survey data at station 4 were recorded. The dashed lines in figure 2 represent the mass-averaged performance of the original rotor as reported in references 3 and 4.

3988

Three important observations can be made concerning the data given in figure 2. First, at high rotational speeds, the peak efficiencies decreased considerably with the 6° reduction in blade angle. Second, as expected, the low-blade-angle rotor passed a higher maximum weight flow than the original rotor. (The occurrence of vertical pressure-ratio and efficiency characteristics at the maximum weight flow is taken as a sign of rotor choking.) Third, there was a marked change in the stalled or low-flow performance characteristics of the low-blade-angle rotor as the speed was increased.

The efficiency variations are discussed later; however, the observations on the maximum weight flow and the stalled performance characteristics deserve some amplification at present.

Maximum weight flow. - An 8-percent increase in maximum (choke) weight flow accompanied the 6° reduction in blade angle at a tip speed of 1000 feet per second (fig. 2(b)). At 1100 feet per second, the increase was 7 percent (fig. 2(a)). An increase in weight flow was expected; however, it is of interest to compare the measured increase with a value calculated from the velocity diagrams assuming no variation with blade angle of the incidence angle at which the rotor chokes. For equal tip-section choking incidence angles, at a corrected tip speed of 1100 feet per second the maximum weight flow should increase 14 percent with the 6° reduction in blade angle. Therefore, the smaller actual increase in flow signifies an increase in incidence angle for rotor choking as the setting angle of these blades is reduced.

Stalled operation of low-blade-angle rotor. - At a fixed rotor speed, some form of compressor blade stall usually occurs at weight flows below the value at which peak total-pressure ratio occurs. Figure 2 shows a variation with tip speed in the performance characteristics for stalled

operation of the low-blade-angle rotor. The pressure ratio and efficiency varied continuously with weight flow at speeds of 900 feet per second and lower; however, at 1000 and 1100 feet per second, the rotor exhibited different characteristics. An abrupt drop in pressure ratio and (to a lesser degree) efficiency occurred for a reduction in weight flow below the value for peak pressure ratio. These changes in performance characteristics with tip speed are probably related to the stall characteristics (ref. 10), which were not studied in detail in these tests. Reference 10 associates a progressive stalling of the blades (a progressive stall starts in a confined region along the span, and the region grows in size as the flow is reduced) with a continuous performance characteristic and states that a full-span stall occurs with an abrupt drop in pressure ratio.

3888

Radial Variations of Rotor-Inlet Conditions

Rotor-inlet conditions (station 3) were computed assuming a zero tangential component of the inlet absolute velocity. No inlet guide vanes were used, and preliminary survey data indicated no prewhirl.

The measured radial variation of inlet absolute Mach number M_3 is plotted in figure 3 as the ratio of Mach number to mean-radius Mach number $M_3/M_{3,m}$. Data are given for several weight flows at corrected rotor tip speeds of 900, 1000, and 1100 feet per second. The inlet Mach number variation is similar for all conditions except for low weight flows at 900 feet per second. The data show a change with speed in the inlet Mach number profile for stalled operation of the rotor. This observation, along with the over-all performance characteristics (fig. 2) and the rotor-outlet conditions (to be discussed later), suggests that a tip-region stall occurs at a tip speed of 900 feet per second and a full-span stall occurs at 1100 feet per second. However, the data for operation at 1000 feet per second indicate that a full-span or a partial-span stall might be present.

Inlet relative air angles β_3' (measured from the axis of rotation) are plotted against radius in figure 4 for several weight flows at corrected tip speeds of 900, 1000, and 1100 feet per second. Blade inlet angles $\varkappa_3$ are also given to indicate incidence angles for particular operating conditions.

Figure 5 shows rotor-inlet relative Mach number M_3' again for several weight flows at 900, 1000, and 1100 feet per second. Relative Mach numbers were supersonic over 50 percent of the blade span for operation

at a corrected rotor tip speed of 1100 feet per second. The rotor tip experienced relative inlet Mach numbers of approximately 1.2.

Radial Variation of Rotor-Outlet Conditions and Blade-Element Characteristics

Radial variations of total-pressure ratio P_4/P_1, blade-element adiabatic efficiency η_b, work coefficient $\Delta H/U_t^2$ (computed from measured temperature rise), and relative total-pressure-loss coefficient $\bar{\omega}'$ are presented in figure 6. Also given are the variations with radius of the absolute discharge Mach number M_4, the relative discharge Mach number M_4', the absolute discharge angle β_4, and the deviation angle δ°. These data are shown for several weight flows at corrected tip speeds of 900, 1000, and 1100 feet per second.

At a tip speed of 900 feet per second (fig. 6(a)) four operating conditions are shown, the maximum weight flow, a weight flow at which the rotor operates near both peak efficiency and peak pressure ratio, and two weight flows in the stalled region of operation. Shown at both 1000 and 1100 feet per second speeds are operating conditions at maximum weight flow, near maximum efficiency, near peak pressure ratio, and at low flow and low efficiency (stalled operation).

At weight flows lower than the peak-efficiency condition at 900 feet per second (fig. 6(a)), large increases in tip-region losses occurred with decreasing weight flow; whereas, the hub region experienced no consistent change in loss with weight flow. These phenomena are taken as further evidence of the tip-region stall postulated from the over-all performance characteristics (fig. 2(c)) and the inlet flow distributions (fig. 3(a)). The high tip-region losses reduced the tip-region total-pressure ratio from the level attained at peak-efficiency (peak pressure ratio, in this case) operation of the rotor. Note that the increase in tip-region losses was large enough to produce the decrease in total-pressure ratio in spite of an increasing work coefficient. The increases in tip-region losses also caused increases in absolute flow angle and decreases in the outlet Mach numbers in the tip region.

At a corrected tip speed of 1000 feet per second (fig. 6(b)), the losses at the three higher weight flows were about equal; however, an increase in loss in the tip region occurred as the flow was reduced to the value for which stall occurred. At 1100 feet per second, the losses for all radii increased above the peak-pressure-ratio losses when the rotor operated in a stalled condition ($w\sqrt{\theta}/\delta A_F$ = 30.8 (lb/sec)/sq ft). Since there is no important change in the variation of loss with radius as the rotor goes into stalled operation at 1100 feet per second, a

3888

full-span stall probably occurs at this speed. The radial variations in losses at 1000 feet per second suggest a tip-region stall, although the over-all performance characteristics (fig. 2) and the inlet absolute Mach number variations (fig. 3) for this speed indicate a full-span stall.

As shown in figure 6, tip-region losses were the largest found anywhere on the blade span, and they increased with speed more than the losses at the other radial positions. The high losses at 1100 feet per second (fig. 6(c)) caused a different radial variation in total pressure from that for the lower speeds. That is, the maximum of the pressure ratio - radius curves at 900 and 1000 feet per second (for peak efficiency) occurred about 1/2 inch from the outer wall. At 1100 feet per second the maximum occurred between 1 and $1\frac{1}{2}$ inches from the outer wall.

3888

Weight-Flow Distributions

CN-2

Radial variations of the elemental weight flow $\rho V_z r$ at the rotor-inlet and -outlet stations are compared in figures 7(a), (b), and (c) for tip speeds of 900, 1000, and 1100 feet per second, respectively. Data are given for operation of the rotor near peak efficiency and in stall. This information shows the radial shifts of the air in flowing through the rotor, as indicated by a comparison of upstream and downstream data.

The abscissas and ordinates used in the plots of figure 7 were chosen to eliminate differences in passage height from the comparisons of inlet and outlet weight-flow distributions. The abscissas are percent of passage height x, where

$$x = \frac{r - r_h}{r_t - r_h}$$

The dimensionless ordinates $\frac{\rho V_z r(r_t - r_h)}{\rho_{a,1} a_{a,1} r_t^2}$ were chosen with the aid of the equation for integrated weight flow

$$w = 2\pi \int_{r_h}^{r_t} \rho V_z r \, dr = 2\pi \int_{r_h}^{r_t} \rho V_z r(r_t - r_h) \, dx$$

The comparisons of inlet and outlet weight-flow distributions at peak efficiency in figure 7 show a progressively larger shift in flow toward the hub as the speed increased. A similar observation could also be made from the axial-velocity-ratio variations in figure 8. (The original rotor did not produce a shift in flow.) The shift in flow and the change with speed can be explained on the basis of the radial

variation of the losses and work coefficient (fig. 6) and the requirements of radial equilibrium (ref. 11). Similar shifts in flow were observed at choked operation.

Comparison of the flow distributions for stalled operation with those for peak-efficiency operation gives some information on the discussion of partial-span and full-span stalling of the rotor. At a corrected tip speed of 900 feet per second (fig. 7(a)), the data imply a tip-region stall, because a greater shift in flow toward the hub occurred at stalled operation than at peak-efficiency operation of the rotor. At 1100 feet per second, however, stalling of the rotor evidently made no change in the flow shift as might be expected if a full-span stall occurred.

3888

Blade-Element Performance

Definition of blade element. - The blade elements are arbitrarily defined as in references 3 and 4, which give the performance of the original version of the present low-blade-angle rotor. That is, blade elements are taken as those cross sections of the blade that lie on conical stream surfaces of revolution, and the stream surfaces are assumed to divide the passage height into equal percentage radial increments upstream and downstream of the blade row. Geometries of the low-blade-angle rotor and the original rotor are given for several radial positions in table I.

As may be seen from the weight-flow-distribution curves (fig. 7), it cannot be presumed that the air in passing through the rotor follows the stream surfaces used to define the blade elements. For this reason, the blade-element data given herein are incorrect in the strict sense of a blade-element theory, because the actual flow occurs along blade elements having a geometry different from that assumed. However, the data are useful, and the blade-element data of the low-blade-angle rotor can be compared directly with the original rotor data under the assumption of similar element geometries. Some of the blade-element parameters, in particular the incidence and deviation angles, are not greatly sensitive to errors in the selection of blade elements. In addition, the error in the loss coefficients caused by the placement of the blade elements is small, because the inlet total pressure and temperature do not vary with radius.

Presentation of blade-element data. - The blade-element characteristics for the low-blade-angle rotor are shown in figure 8 for four blade elements located 11, 17, 50, and 83 percent of the passage height from the outer wall. Data are given for five corrected tip speeds 600, 800, 900, 1000, and 1100 feet per second. The characteristics shown are the variations with incidence angle of the relative total-pressure-loss coefficient $\bar{\omega}'$, deviation angle δ°, inlet relative Mach number M_3', axial velocity ratio $V_{z,4}/V_{z,3}$, diffusion factor D (ref. 12), work coefficient $\Delta H/U_t^2$ (nondimensional temperature rise), and blade-element adiabatic efficiency η_b.

[redacted]

Tip section. - As shown in figures 8(a) and (b), as speed and relative inlet Mach number increased, diffusion factor D, work coefficient $\Delta H/U_t^2$, and losses $\bar{\omega}'$ increased and axial velocity ratio $V_{z,4}/V_{z,3}$ decreased. At the minimum-loss incidence angle for a corrected tip speed of 1100 feet per second, the loss coefficient $\bar{\omega}'$ was 0.35 for the 11-percent blade element (fig. 8(a)). At this condition, the inlet relative Mach number was 1.2, the diffusion factor 0.65, and the axial velocity ratio 0.71.

3888

Minimum-loss incidence angles increased as inlet relative Mach number (tip speed) increased. At 1100 feet per second, the minimum-loss incidence angle was about 5.5° for the 11-percent blade element (fig. 8(a)) compared with a value of 2° or 3° for 600 feet per second.

CN-2 back

Measured deviation angles in the minimum-loss region of operation increased somewhat with increasing speed level at the 11-percent blade element (fig. 8(a)), but little variation with speed occurred for the 17-percent blade element (fig. 8(b)). The variations in deviation angle δ° with speed may be obtained because of the large changes in losses and axial velocity ratio with speed (refs. 13 and 14).

Mean section. - Minimum-loss coefficients at the mean section (fig. 8(c)) were low for all speeds, and they increased slightly with increasing inlet relative Mach number (tip speed). However, even at an inlet relative Mach number of 1.01 (1100 ft/sec) the losses were fairly low.

Again, an increase in the minimum-loss incidence angle with inlet relative Mach number (tip speed) is observed. A marked shift in the loss curve toward high incidence angles is seen at 1100 feet per second with no accompanying increase in the minimum-loss level. This loss phenomenon may be related in some way to increase in axial velocity ratio for operation between 1000 and 1100 feet per second. The increase in axial velocity ratio results from the shift in flow toward the hub, as discussed earlier (fig. 7).

Deviation angles for the mean section increased with increasing speed up to a tip speed of 1000 feet per second. Then, as the tip speed was increased to 1100 feet per second, δ° decreased. This phenomenon, too, is probably related to the change in axial velocity ratio mentioned previously.

Hub section. - Loss data for the hub section (fig. 8(d)) are scattered; however, the losses were generally low. Except for operation at a tip speed of 1100 feet per second, the hub section had a wide incidence-angle range. Variations with speed of losses $\bar{\omega}'$, diffusion factor D, axial velocity ratio $V_{z,4}/V_{z,3}$, and work coefficient $\Delta H/U_t^2$ were less than at the rotor tip.

As at the mean section, hub-section deviation angles increased with increasing speed up to a tip speed of 1000 feet per second and then decreased as the speed was increased to 1100 feet per second.

[redacted]

COMPARISON OF LOW-BLADE-ANGLE AND ORIGINAL ROTOR BLADE-ELEMENT DATA

Blade-element data are compared for blade sections near the hub and the mean section and for two sections near the tip in figure 9. The relative total-pressure-loss coefficient $\bar{\omega}'$, the axial velocity ratio $V_{z,4}/V_{z,3}$, the diffusion factor D, the deviation angle δ°, and the relative inlet Mach number M_3' are plotted against incidence angle i. Data are given for tip speeds of 900, 1000, and 1100 feet per second for the low-blade-angle rotor and 1000 and 1100 feet per second for the original rotor.

3888

The data for the original rotor were taken from reference 4, which gives the performance of the original rotor followed by a set of high-turning stator blades. The hub contour downstream of the rotor was modified for the tests reported in reference 4 and differs from the hub contour of the low-blade-angle rotor. The difference in hub contour might influence performance comparisons at the hub, but it would not affect the comparisons at the mean and tip sections.

It is of interest to note that relative inlet Mach numbers M_3' are nearly equal for the original rotor operated at a tip speed of 1000 feet per second and for the low-blade-angle rotor at 900 feet per second. Relative inlet Mach numbers are also similar on the original and low-blade-angle rotors for tip speeds of 1100 and 1000 feet per second, respectively. This factor makes it possible to compare the performance of blade elements at equivalent inlet relative Mach number levels for the two different blade angles.

The discussion is concerned mainly with the measured loss coefficients, and the tip-region performance is considered first.

Tip Region

The tip-region performance of the original and the low-blade-angle rotors is compared by considering the blade-element performance of two sections located 11 percent and 17 percent of the passage height away from the outer wall (figs. 9(a) and (b), respectively). The discussion will, in general, apply to both blade elements.

Several observations can be made concerning the data in figure 9(a). At a given tip speed, higher minimum loss coefficients were measured for the low-blade-angle rotor than for the original rotor, and considerably higher minimum-loss incidence angles occur for the low-blade-angle rotor.

For operation of both rotors at equivalent inlet relative Mach numbers in the vicinity of 1.0, the loss - incidence-angle curves are nearly

coincident. At the next higher equal inlet relative Mach number level (approx. 1.1), the losses at high incidence angles are equal for both rotors (fig. 9(a)). However, the minimum-loss level and the incidence angle for minimum-loss operation are both higher for the low-blade-angle rotor than for the original rotor. These observations and the general appearance of the loss curves (at an inlet relative Mach number of 1.1) suggest that lower losses would occur at the tip section of the low-blade-angle rotor if the rotor could be operated at incidence angles below those observed.

3888

It has sometimes been stated that blade-element losses for operation at minimum-loss incidence angle depend on the inlet relative Mach number, the blade loading, and, perhaps, the ratio of outlet to inlet axial velocity. In a particular compressor investigation, the influence of each of these factors is difficult to determine unless some sort of comparison with other data can be made. If the diffusion factor D of reference 12 is taken as a measure of the blade loading at minimum-loss incidence angle, a study of the individual factors that influence losses may be possible through a comparison with the data given in reference 12.

Diffusion factors and surface Mach numbers. - In an attempt to separate some of the factors that may influence the measured tip-section losses, the relative total-pressure-loss coefficient $\bar{\omega}'$ was plotted against the diffusion factor D as shown in figure 10. Data for the blade element located 11 percent of the passage away from the outer wall were chosen for this plot so that a comparison with the correlation of reference 12 (indicated by the dashed lines) could be made. Figure 10 includes data near minimum-loss operation for the original and the low-blade-angle rotors and similar information for tip sections (10% to 15% of passage height from the outer wall) of transonic-compressor rotors reported in references 4, 7, 9, and 15.

As reported in reference 4, the data for the tip section of the original rotor fall within the band of data determined in reference 12. However, the losses at a corrected tip speed of 1100 feet per second are near the upper limit of the band of data (fig. 10). Only at speeds below 1000 feet per second do the losses of the low-blade-angle rotor agree with the loss - diffusion-factor correlation of reference 12. The minimum loss coefficient at a tip speed of 1000 feet per second is slightly above the band; whereas the losses at 1100 feet per second for the low-blade-angle rotor are much farther away.

[redacted]

Loss coefficients for three other transonic-compressor rotors (refs. 7, 9, and 15) also fall above the upper limit line of the correlation of reference 12 (fig. 10). The important fact is that for certain designs and geometries the blade loading as given by the diffusion factor is not the only parameter that influences the losses. Inlet relative Mach number by itself also does not provide correlation of the loss data, because the loss levels and the margin by which the measured losses exceed the band of data in figure 10 cannot be explained on the basis of the inlet relative Mach number level.

3888

It was speculated in reference 7 that the peak value of suction-surface Mach number is an important factor to be considered in regard to losses. This concept was based on a simplified picture of the shock waves occurring in a blade passage. It is assumed that a detached bow wave occurs ahead of the leading edge of a blade and that this shock wave strikes the suction surface of the adjacent blade some distance back from the leading edge. The shock wave introduces free-stream total-pressure losses and affects the characteristics of the boundary layer on the suction surface. A rough measure of the importance of the shock wave can be determined from the peak suction-surface Mach number, which is that value of suction-surface Mach number immediately upstream of the shock wave. The magnitude of the peak suction-surface Mach number can be approximated from the inlet relative Mach number and the amount of turning that occurs along the suction surface up to the assumed intersection of the shock wave with the suction surface. Peak suction-surface relative Mach numbers were computed for the low-blade-angle and original rotors using Prandtl-Meyer expansion equations. A shock wave for each rotor was assumed as shown in reference 7, and the computed values for peak suction-surface relative Mach number M_s' are given in the table in figure 10.

A peak surface Mach number of 1.67 was computed for the low-blade-angle rotor operating at a tip speed of 1100 feet per second. It is felt that a shock wave at this Mach number level certainly will influence the boundary-layer growth on the blade surfaces. In addition, the loss in total pressure across the shock wave could contribute a sizable amount to the over-all measured losses. The lower peak suction-surface Mach numbers for the original rotor indicate smaller shock-wave effects.

Suction-surface Mach numbers computed for the rotors of references 7, 9, and 15 are also given in figure 10. It can be seen that all the loss values that fall above the band of data by a large amount represent cases in which the computed peak suction-surface Mach numbers were about 1.70. In fact, a line parallel to the original band of data can be drawn through the points in question in figure 10. Thus, it can be concluded that the peak suction-surface Mach number level has some effect on the losses. The exact nature and magnitude of the effect is at present unknown.

Another interesting point is also shown by the data in figure 10. Values of the ratio of rotor-outlet to -inlet axial velocity, shown in the table, range from 0.73 up to 1.10 for the rotors having peak suction-surface Mach numbers of about 1.70, and no independent effect of axial velocity ratio is evident. That is, the loss data, which admittedly are limited, correlate only on the basis of peak suction-surface Mach number and diffusion factor. Therefore, it appears that the only influence of axial velocity ratio on losses is its effect on the value of diffusion factor D. The high losses observed in the tip region of the low-blade-angle rotor, therefore, can be traced to high values of diffusion factor D and peak suction-surface Mach number.

3888

Minimum-loss incidence angle. - As mentioned earlier, high values of minimum-loss incidence angle were observed at high inlet relative Mach numbers for the low-blade-angle rotor. High incidence angles, of course, produce high values of suction-surface Mach number, which in turn affect losses. Increases in minimum-loss incidence angle with increasing inlet relative Mach numbers have been observed in other transonic-compressor investigations (e.g., refs. 4 and 9), and a small increase in incidence angle due to the change in blade angle is indicated by low-speed two-dimensional-cascade data (ref. 16). It is desirable to compare the low-blade-angle rotor data with the previous results to discover whether the observed minimum-loss incidence-angle levels and trends for the low-blade-angle rotor are what might be expected. Such a comparison is given in figure 11, the data of which are reproduced from figure 13 of reference 9, with added data for the original and the low-blade-angle rotors discussed in this report. Rotor reference incidence angle (minimum-loss incidence angle) minus cascade-rule incidence angle (ref. 16) is plotted against inlet relative Mach number.

The significant feature of the comparison in figure 11 is that, for Mach numbers above 1.05, a greater variation of minimum-loss incidence angle with inlet Mach number occurs for the low-blade-angle rotor than for the original rotor (ref. 4) and the data of reference 9. As a result, the minimum-loss incidence angle for the low-blade-angle rotor operated at 1100 feet per second is high compared with previous data. Therefore, it appears that some factors other than inlet relative Mach number must be considered in a correlation of measured minimum-loss incidence angles.

Hub and Mean Sections

Losses. - Near the hub (fig. 9(d)), the losses for the original rotor (ref. 4) are generally higher than the losses for the low-blade-angle rotor. In other tests of the original rotor (ref. 3) in which the hub contour was identical to the one used with the low-blade-angle rotor, the measured losses near the hub were equal to the losses for the low-blade-angle rotor. None of the usual flow parameters (inlet relative

Mach number, diffusion factor, or axial velocity ratio) provide any apparent explanation of the loss differences. Thus, the difference in loss levels shown in figure 9(d) may be caused by experimental errors or, in some unknown way, by differences in hub contour.

The minimum relative total-pressure-loss coefficients at the mean section (fig. 9(c)) are about equal for both the original and the low-blade-angle rotors.

Choking incidence angles at hub section. - As mentioned earlier in this report, the minimum-loss incidence angles in the tip region were quite high for the low-blade-angle rotor for high-speed operation, and the variation of minimum-loss incidence angle with inlet relative Mach number was greater than for a previous correlation (fig. 11). Since the minimum-loss incidence angles (for high inlet relative Mach numbers) usually are 1° or 2° greater than the incidence angles at which the rotor chokes, an analysis of the rotor choking phenomenon may provide a reason for the occurrence of high minimum-loss incidence angles in the tip region of the low-blade-angle rotor compared with the original rotor.

Rotor choking occurs when the over-all performance characteristics (fig. 2) exhibit a vertical total-pressure-ratio line at the maximum weight flow for a given rotational speed. Under such operating conditions, the air properties at the rotor outlet vary with a change in back pressure, but no alteration of the inlet flow occurs. Choking of a compressor or turbine rotor or any annular cascade is three-dimensional (ref. 17). That is, each blade element behaves as if it were choked when the blade row chokes in spite of any two-dimensional-cascade data or analysis that might indicate differently. Experimental data seem to support this position in that, for constant inlet conditions, the rotor-outlet properties at all radial positions vary with back pressure in the choked operating region.

Design of a compressor blade row, of course, requires information regarding the choking incidence angles. Sources of such data might be two-dimensional-cascade data, rotor blade-element data, or some analytical method such as a one-dimensional channel flow calculation. Each source of choking incidence angles will sometimes fail to supply correct values, depending on the particular compressor design problem, because of the three-dimensional nature of the choking phenomenon. The failure of an analytical method to provide correct choking incidence angles is shown through a comparison of low-blade-angle-rotor choking incidence angles at the hub with values determined from a channel flow calculation. By including the original rotor data in the comparison, a three-dimensional flow factor important in rotor choking is illustrated.

3886

[redacted]

Choking incidence angles were computed by assuming a one-dimensional isentropic channel flow for the hub element (inlet radius, 5.12 in.). The channels were assumed to choke with a constant Mach number of 1.0 across the passage at the minimum spacing between two adjacent blades (measured from blade layouts). The reduction of stream-tube height from the inlet of the blade to the throat caused by the hub contour was included in the calculation according to the following simplified concept:

$$\frac{\Delta b_{th}}{\Delta b_3} = \frac{r_t - r_{h,th}}{r_t - r_{h,3}}$$

where the ratio of stream-tube height at the throat to that at the blade inlet $\Delta b_{th}/\Delta b_3$ is assumed equal to the ratio of the annulus heights at the throat and inlet. The results of the calculation are given in the following table along with the hub-element data for the lowest-incidence-angle operation at each speed. Lowest-incidence-angle operation corresponds to the condition of rotor choking as evidenced by the vertical pressure-ratio characteristics at maximum flow (fig. 2).

Rotor	$U_t/\sqrt{\theta}$, ft/sec	Calculated		Measured	
		Choking i, deg	M'_3	Choking i, deg	M'_3
Original	1000	2.4	0.77	2.6	0.77
	1100	3.7	.83	3.7	.83
Low-blade-angle	900	2.6	0.78	3.5	0.76
	1000	4.4	.84	5.5	.82
	1100	5.4	.91	6.9	.87

The agreement between computed and measured choking incidence angles for the original rotor is excellent; however, a certain amount of good fortune must be admitted in view of the approximations and assumptions used in the calculations. For the low-blade-angle rotor there is a difference between measured and computed choking incidence angles, and the difference increases with increasing speed. The important factor is not that excellent agreement was obtained for the original rotor but rather that the accuracy of the choking calculation differs for each compressor. The latter observation is construed as an indication of some changes in the flow characteristics with blade angle which are not included in the simple choking analysis.

The most obvious flow characteristic to consider here is the radial shift in flow toward the hub that occurred in the low-blade-angle rotor and not in the original rotor. The observations on the radial shift in flow could be taken as reasons for the change in the agreement between computed and measured hub-section choking incidence angles with blade

angle, because a shift in flow toward the hub would vitiate the stream-tube height relation given previously. Since both the difference between calculated and measured choking incidence angles and the radial shift in flow toward the hub increase with increasing speed, further importance may be attached to the influence of the flow shift in the choking phenomenon.

A radial shift in flow toward the hub also means that a reduced weight flow is being handled in the tip region, and the entire rotor must choke at lower weight flows (higher incidence angles) than would occur with no flow shift. Thus, it appears that the high minimum-loss incidence angles in the tip region of the low-blade-angle rotor can be traced to the shift in flow toward the hub. The observed increase in the flow shift with increasing speed may also be the reason for large variation of minimum-loss incidence angle with inlet relative Mach number compared with the correlation of reference 9 (fig. 11).

3886

CONCLUDING REMARKS

The data given in this report suggest that the magnitude of the peak suction-surface Mach number should be considered, along with the blade loading, in correlating and predicting blade-element losses for high inlet relative Mach numbers. At peak suction-surface Mach numbers of 1.70, shock losses and effects of the shock wave on the blade boundary layers are large enough to cause measured blade-element losses to fall above a previous correlation of losses with diffusion factor (a measure of blade loading). Therefore, if low losses are required in a transonic-compressor rotor, the design of the rotor should result in low blade loadings and low suction-surface Mach numbers. In order to achieve low suction-surface Mach numbers in blade rows designed for high inlet relative Mach numbers, it will be necessary to employ blade sections having nearly straight suction surfaces over the forward portion of the blade.

Another conclusion apparent from this data is that choking incidence angles for a rotor depend on the radial shifts in the flow as it passes through the blade row. This factor points to the three-dimensional nature of choking in an annular cascade.

This report has also shown some rather large effects of a 6° reduction in blade-setting angle on the performance of a compressor rotor. Basically, this investigation did not illustrate solely the effects of blade-angle changes; instead, it demonstrated the sensitivity of the performance of a highly loaded transonic compressor to variations in the flow characteristics. The data show that the tip section, for this type of compressor, has the greatest effect of any section on the over-all performance.

The concept of sensitivity can be explained by a simplified reconstruction of the high-speed performance of the low-blade-angle rotor based on the original rotor performance and the data and ideas given herein. The reduction in blade angle caused high blade loadings, high inlet relative Mach numbers, and high peak suction-surface Mach numbers at the tip section, compared with the original rotor. (The original rotor was highly loaded itself.) These factors caused increased tip-section losses, while the hub and mean section losses did not change greatly from those for the original rotor. Thus, the low-blade-angle rotor operated with a steeper radial variation of losses than the original rotor. Radial equilibrium then required a change in the radial variation of rotor-outlet axial velocity with blade angle. Comparatively low axial velocities occurred in the tip region, which further increased loading and losses.

3888 CN-3 back

In addition, the high tip-section losses, through the axial velocity variation, produced a radial shift in the flow toward the hub, and the result was high values of incidence angle for rotor choking. These high incidence angles then caused higher tip-section losses through the mechanism of increased suction-surface Mach numbers and shock effects. Thus, the sensitivity arises through a compounding of many effects. The blade-angle change had a large influence on the over-all performance because the original rotor was highly loaded. In addition, the supersonic inlet relative Mach numbers amplified the effects of the blade-angle change.

SUMMARY OF RESULTS

A transonic-compressor rotor was tested at inlet relative Mach numbers up to 1.2 with a tip-section diffusion factor of 0.65 and an axial velocity ratio of 0.71. This rotor was a low-blade-angle version of a compressor tested previously. The following are some of the results of the tests of the low-blade-angle rotor:

1. At high rotational speed, the peak efficiencies decreased considerably with the 6° reduction in blade angle. In addition, the low-blade-angle rotor operated with a greater reduction in peak efficiency with increasing tip speed than did the original rotor.

2. A study of the flow distributions upstream and downstream of the low-blade-angle rotor showed a large shift in flow toward the hub at a tip speed of 1100 feet per second, resulting from the high tip-section losses. The original version did not induce such a shift in flow. The observed shift in flow influences the performance of the low-blade-angle rotor by causing low axial velocity ratios (and high loadings) in the tip region. In addition, the incidence angles at which the rotor chokes appear to be related to the shift in flow.

3. Hub-section losses for the low-blade-angle rotor were low and agreed with some previous compressor data. Low values of minimum loss coefficient at the mean section were observed for inlet relative Mach numbers up to 1.01.

4. Tip-section losses at a tip speed of 1100 feet per second for the low-blade-angle rotor fell above a previous correlation of losses against diffusion factor. Similar results were found for three other compressor rotors. The departure of all these data from the previous correlation could be explained on the basis of high suction-surface Mach numbers.

5. Comparison of the low-blade-angle rotor data with the characteristics of four other compressor rotors showed that axial velocity ratio (outlet over inlet) had no independent effect on the observed losses for axial velocity ratios between 0.73 and 1.10.

3888

Lewis Flight Propulsion Laboratory
National Advisory Committee for Aeronautics
Cleveland, Ohio, October 22, 1956

REFERENCES

1. Lieblein, Seymour, Lewis, George W., Jr., and Sandercock, Donald M.: Experimental Investigation of an Axial-Flow Compressor Inlet Stage Operating at Transonic Relative Inlet Mach Numbers. I - Over-All Performance of Stage with Transonic Rotor and Subsonic Stators Up to Rotor Relative Inlet Mach Number of 1.1. NACA RM E52A24, 1952.

2. Lewis, George W., Jr.: Experimental Investigation of Axial-Flow Compressor Inlet Stage Operating at Transonic Relative Inlet Mach Numbers. II - Blade-Coordinate Data. NACA RM E52C27, 1952.

3. Schwenk, Francis C., Lieblein, Seymour, and Lewis, George W., Jr.: Experimental Investigation of an Axial-Flow Compressor Inlet Stage Operating at Transonic Relative Inlet Mach Numbers. III - Blade-Row Performance of Stage with Transonic Rotor and Subsonic Stator at Corrected Tip Speeds of 800 and 1000 Feet per Second. NACA RM E53G17, 1953.

4. Sandercock, Donald M., Lieblein, Seymour, and Schwenk, Francis C.: Experimental Investigation of an Axial-Flow Compressor Inlet Stage Operating at Transonic Relative Inlet Mach Numbers. IV - Stage and Blade-Row Performance of Stage with Axial-Discharge Stators. NACA RM E54C26, 1954.

5. Robbins, William H., and Glaser, Frederick W.: Investigation of an Axial-Flow-Compressor Rotor with Circular-Arc Blades Operating up to a Rotor-Inlet Relative Mach Number of 1.22. NACA RM E53D24, 1953.

6. Montgomery, John C., and Glaser, Frederick W.: Experimental Investigation of a 0.4 Hub-Tip Diameter Ratio Axial-Flow Compressor Inlet Stage at Transonic Inlet Relative Mach Numbers. II - Stage and Blade-Element Performance. NACA RM E54I29, 1955.

7. Schwenk, Francis C., and Lewis, George W., Jr.: Experimental Investigation of a Transonic Axial-Flow-Compressor Rotor with Double-Circular-Arc Blade Sections. III - Comparison of Blade-Element Performance with Three Levels of Solidity. NACA RM E55F01, 1955.

8. Tysl, Edward R., and Schwenk, Francis C.: Experimental Investigation of a Transonic Compressor Rotor with a 1.5-Inch Chord Length and an Aspect Ratio of 3.0. III - Blade-Element and Over-All Performance at Three Solidity Levels. NACA RM E56D06, 1956.

9. Creagh, John W. R.: Performance Characteristics of an Axial-Flow Transonic Compressor Operating Up to Tip Relative Inlet Mach Number of 1.34. NACA RM E56D27, 1956.

10. Graham, Robert W., and Costilow, Eleanor L.: Compressor Stall and Blade Vibration. Ch. XI of Aerodynamic Design of Axial-Flow Compressors, vol. III. NACA RM E56B03b, 1956.

11. Hatch, James E., Giamati, Charles C., and Jackson, Robert J.: Application of Radial-Equilibrium Condition to Axial-Flow Turbomachine Design Including Consideration of Change of Entropy with Radius Downstream of Blade Row. NACA RM E54A20, 1954.

12. Lieblein, Seymour, Schwenk, Francis C., and Broderick, Robert L.: Diffusion Factor for Estimating Losses and Limiting Blade Loadings in Axial-Flow-Compressor Blade Elements. NACA RM E53D01, 1953.

13. Lieblein, Seymour: Review of High-Performance Axial-Flow-Compressor Blade-Element Theory. NACA RM E53L22, 1954.

14. Schulze, Wallace M., Erwin, John R., and Ashby, George C., Jr.: NACA 65-Series Compressor Rotor Performance with Varying Annulus-Area Ratio, Solidity, Blade Angle, and Reynolds Number and Comparison with Cascade Results. NACA RM L52L17, 1953.

15. Wright, Linwood C., and Wilcox, Ward W.: Investigation of Two-Stage Counterrotating Compressor. II - First-Rotor Blade-Element Performance. NACA RM E56G09, 1956.

16. Lieblein, Seymour: Experimental Flow in Two-Dimensional Cascades. Ch. VI of Aerodynamic Design of Axial-Flow Compressors, vol. II. NACA RM E56B03a, 1956.

17. Stewart, Warner L.: Analytical Investigation of Flow through High-Speed Mixed-Flow Turbine. NACA RM E51H06, 1951.

3888

3888

TABLE I. - ROTOR BLADE-ELEMENT GEOMETRY

Radial position	Percent passage height	Radius, in.		Solidity, σ	Blade angles			
					Original		Reset	
		Inlet	Outlet		Inlet κ_3, deg	Outlet κ_4, deg	Inlet κ_3, deg	Outlet κ_4, deg
Tip	0	8.68	8.68		----	----	----	----
3	11	8.22	8.30	1.29	54.2	32.1	48.2	26.1
4	17	7.97	8.10	1.32	53.5	31.0	47.5	25.0
6	50	6.55	6.93	1.57	48.5	21.7	42.5	15.7
8	83	5.12	5.77	1.91	42.6	7.8	36.6	1.8
Hub	100	4.41	5.19		----	----	----	----

[redacted]

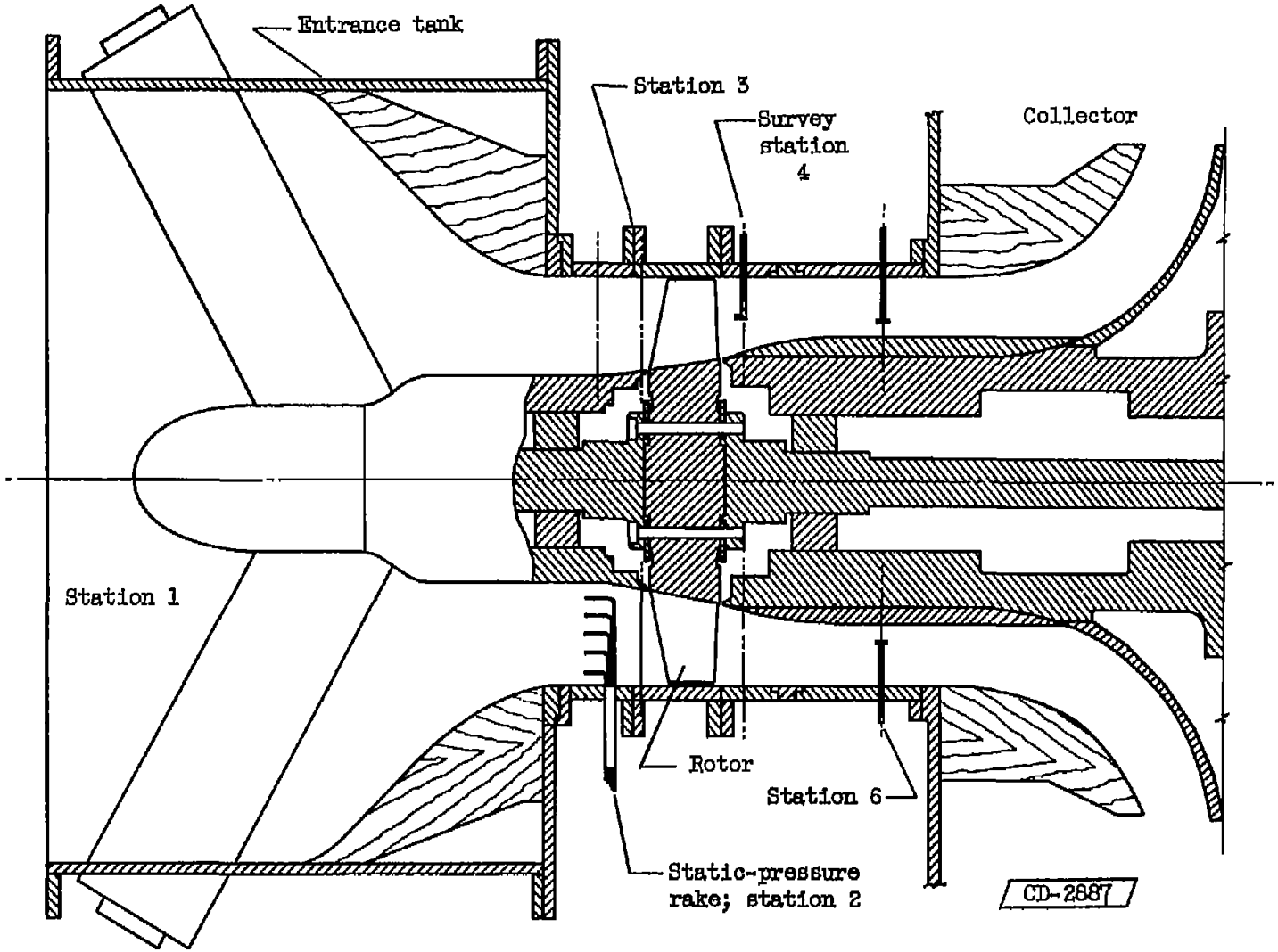

Figure 1. - Schematic diagram of variable-component transonic-compressor test rig.

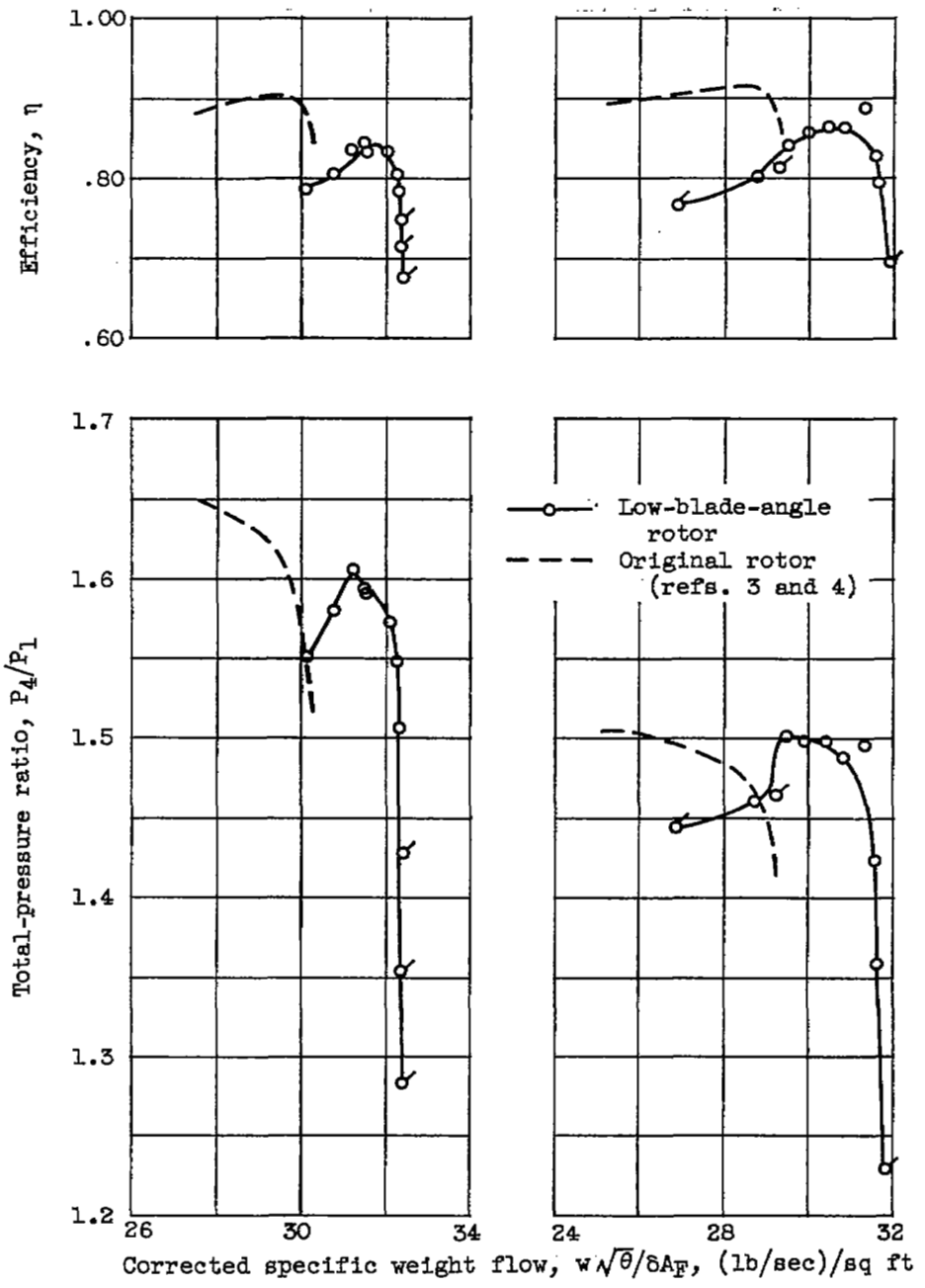

(a) Corrected rotor tip speed, 1100 feet per second.

(b) Corrected rotor tip speed, 1000 feet per second.

Figure 2. - Mass-averaged rotor performance characteristics. (Flags denote area-averaged data.)

3888

[redacted]

3888 CN-4

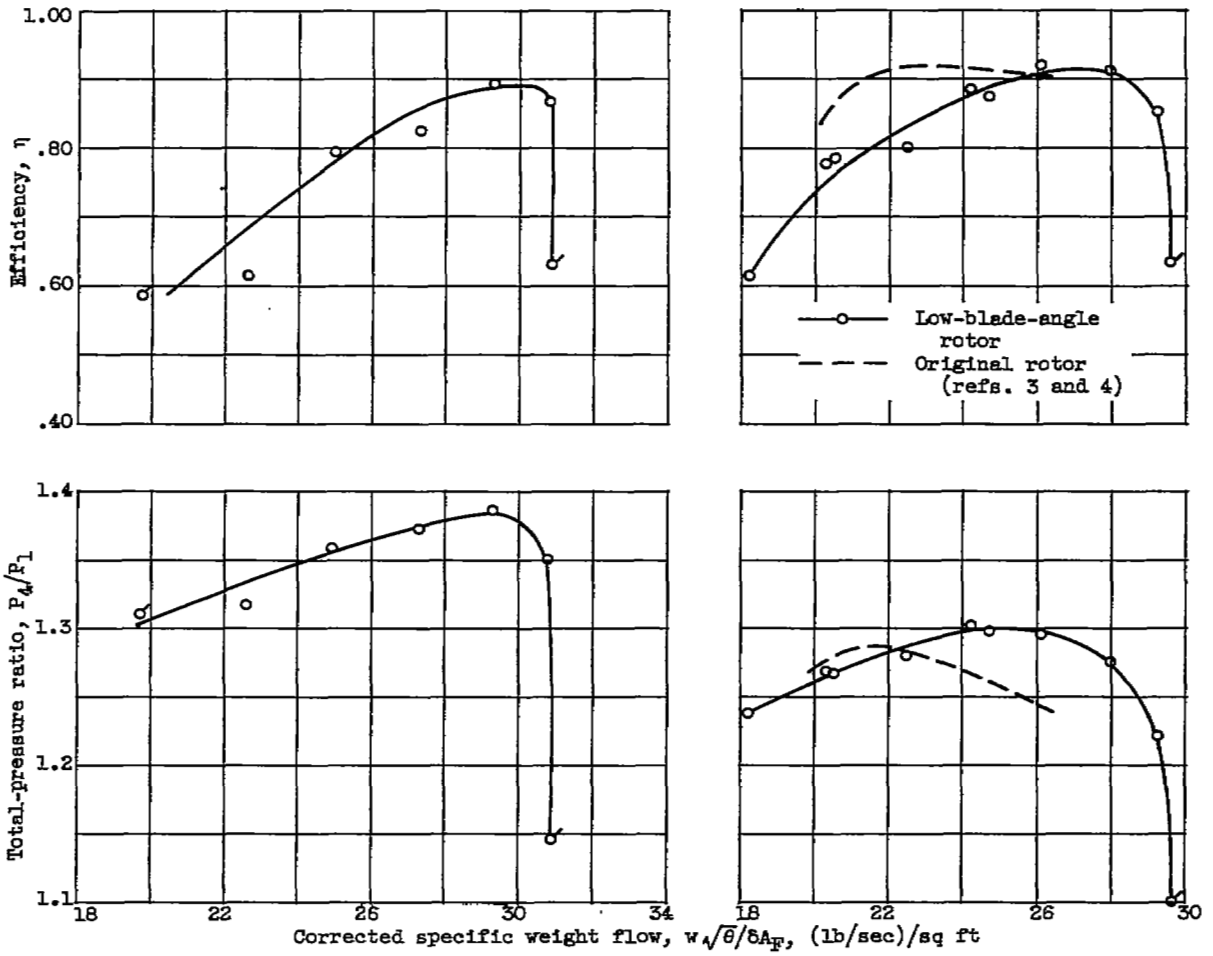

(c) Corrected rotor tip speed, 900 feet per second.

(d) Corrected rotor tip speed, 800 feet per second.

Figure 2. - Continued. Mass-averaged rotor performance characteristics. (Flags denote area-averaged data.)

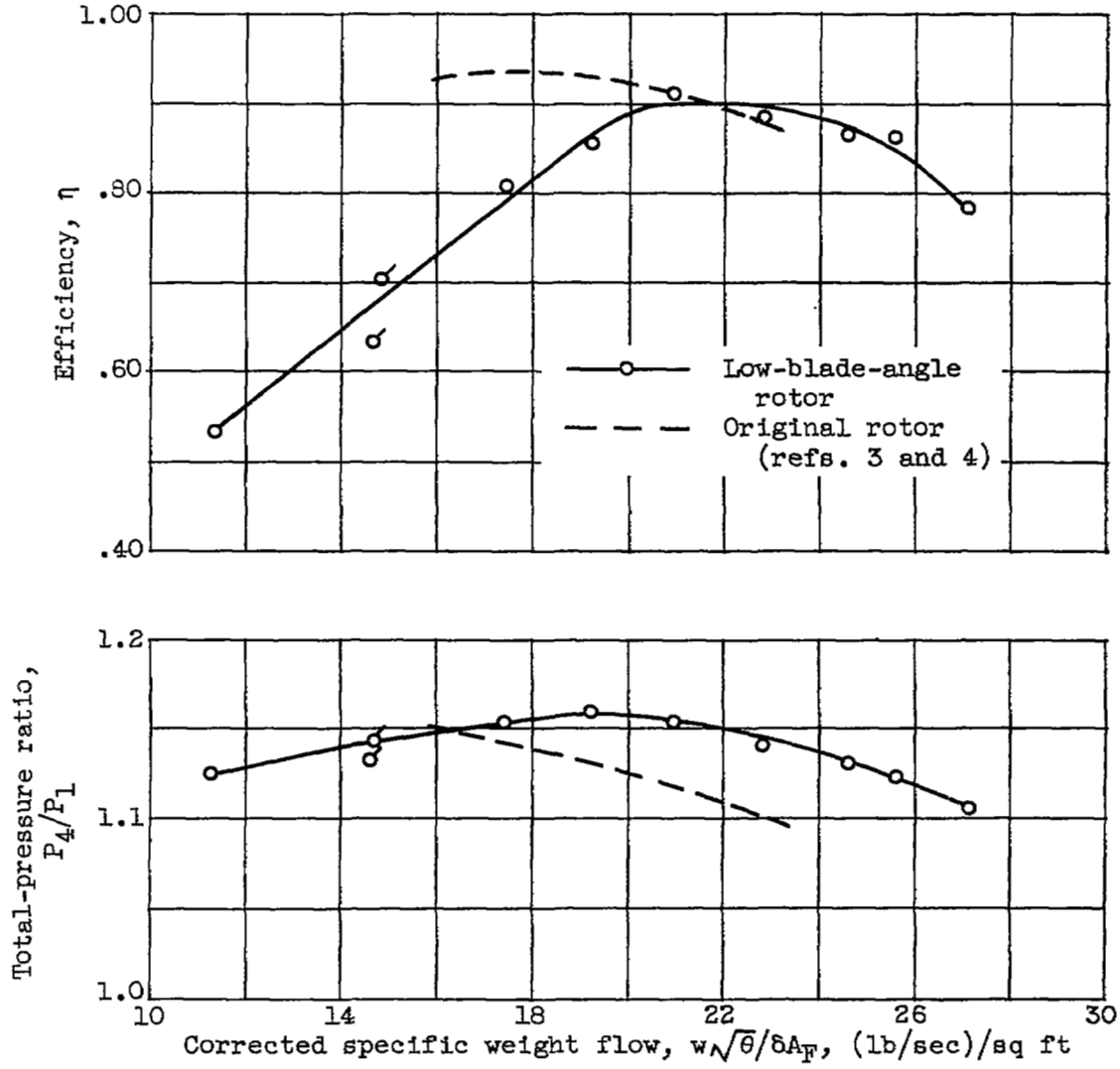

(e) Corrected rotor tip speed, 600 feet per second.

Figure 2. - Concluded. Mass-averaged rotor performance characteristics. (Flags denote area-averaged data.)

3888

3888 CN-4 back

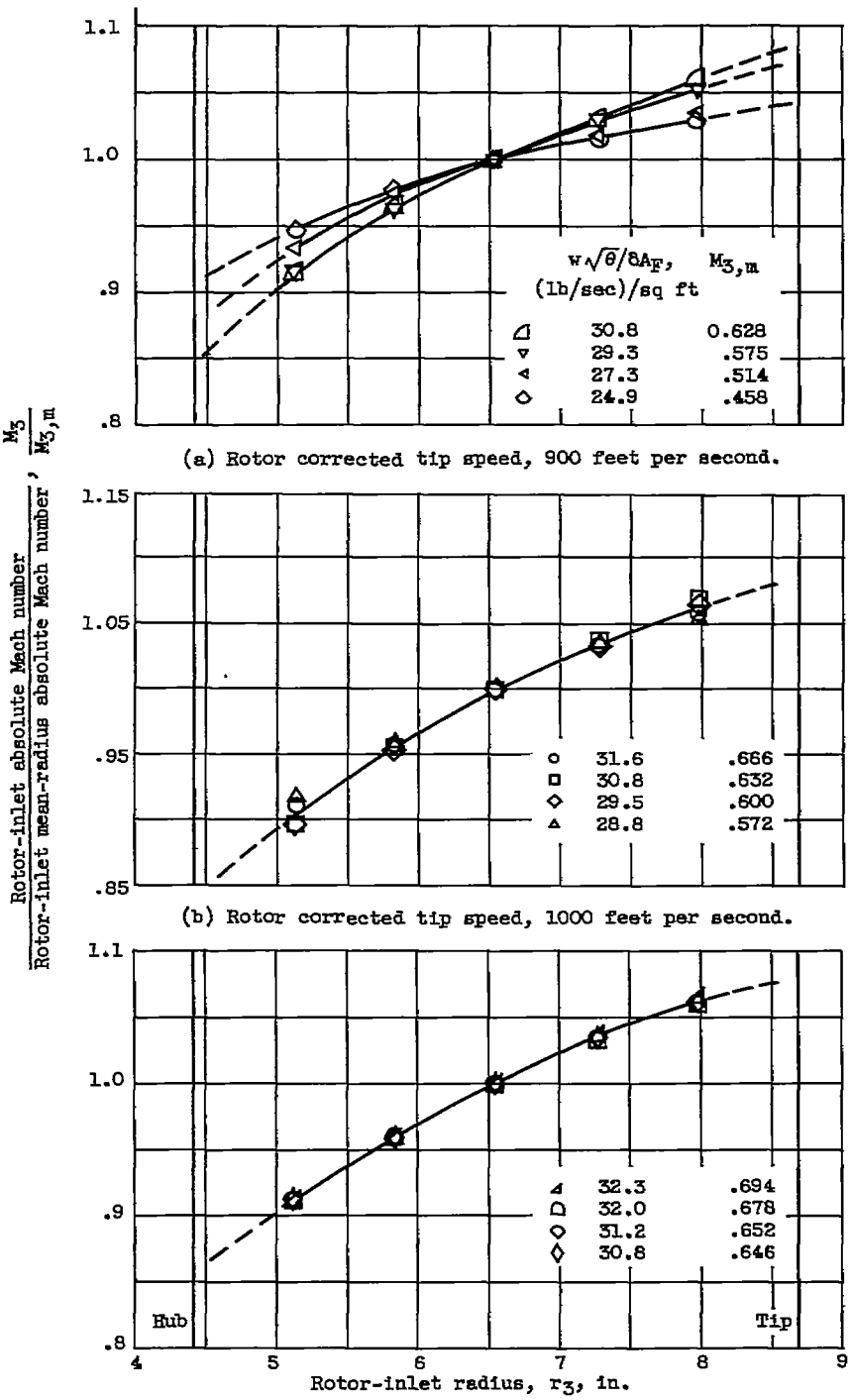

(a) Rotor corrected tip speed, 900 feet per second.

(b) Rotor corrected tip speed, 1000 feet per second.

(c) Rotor corrected tip speed, 1100 feet per second.

Figure 3. - Radial variation of rotor-inlet absolute Mach number (station 3).

[redacted]

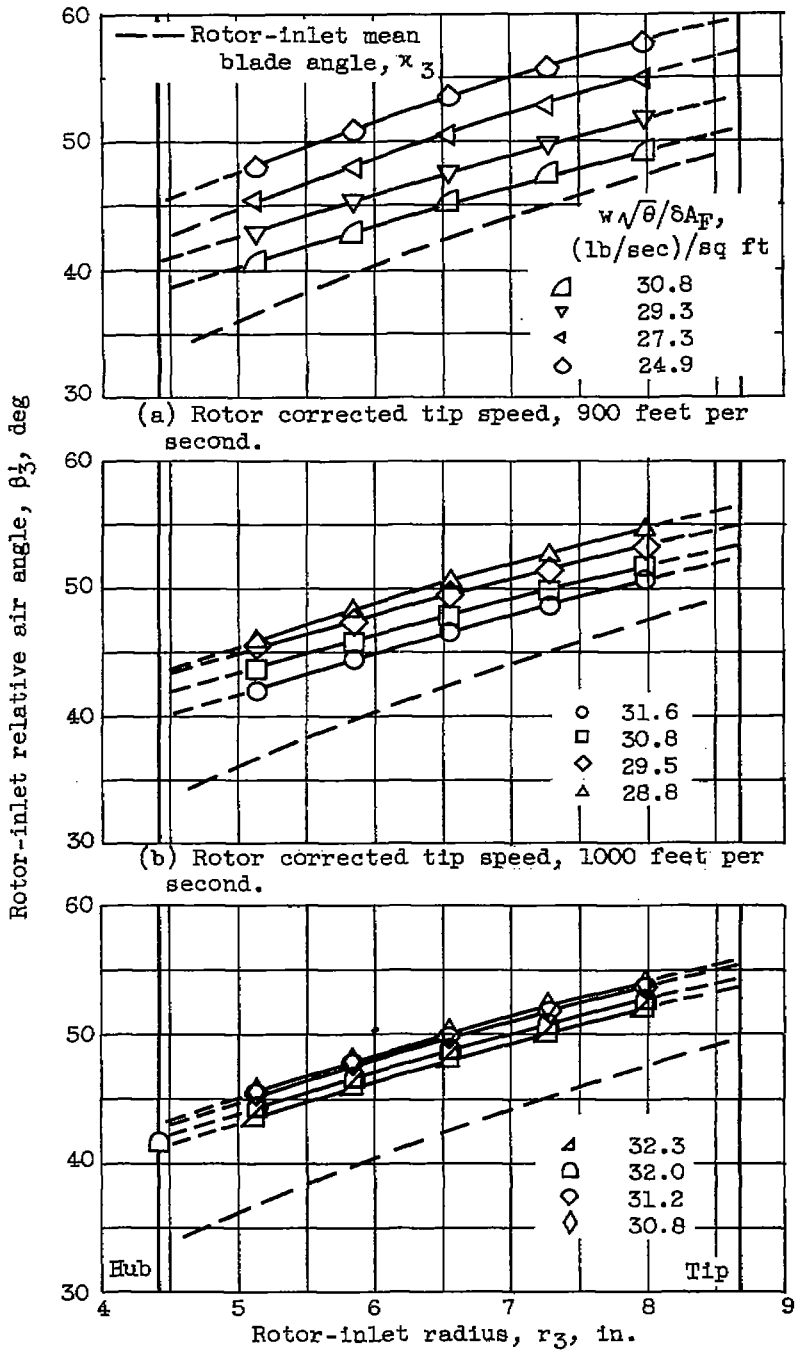

(a) Rotor corrected tip speed, 900 feet per second.

(b) Rotor corrected tip speed, 1000 feet per second.

(c) Rotor corrected tip speed, 1100 feet per second.

Figure 4. - Radial variation of rotor-inlet relative air angles.

3888

[redacted]

3888

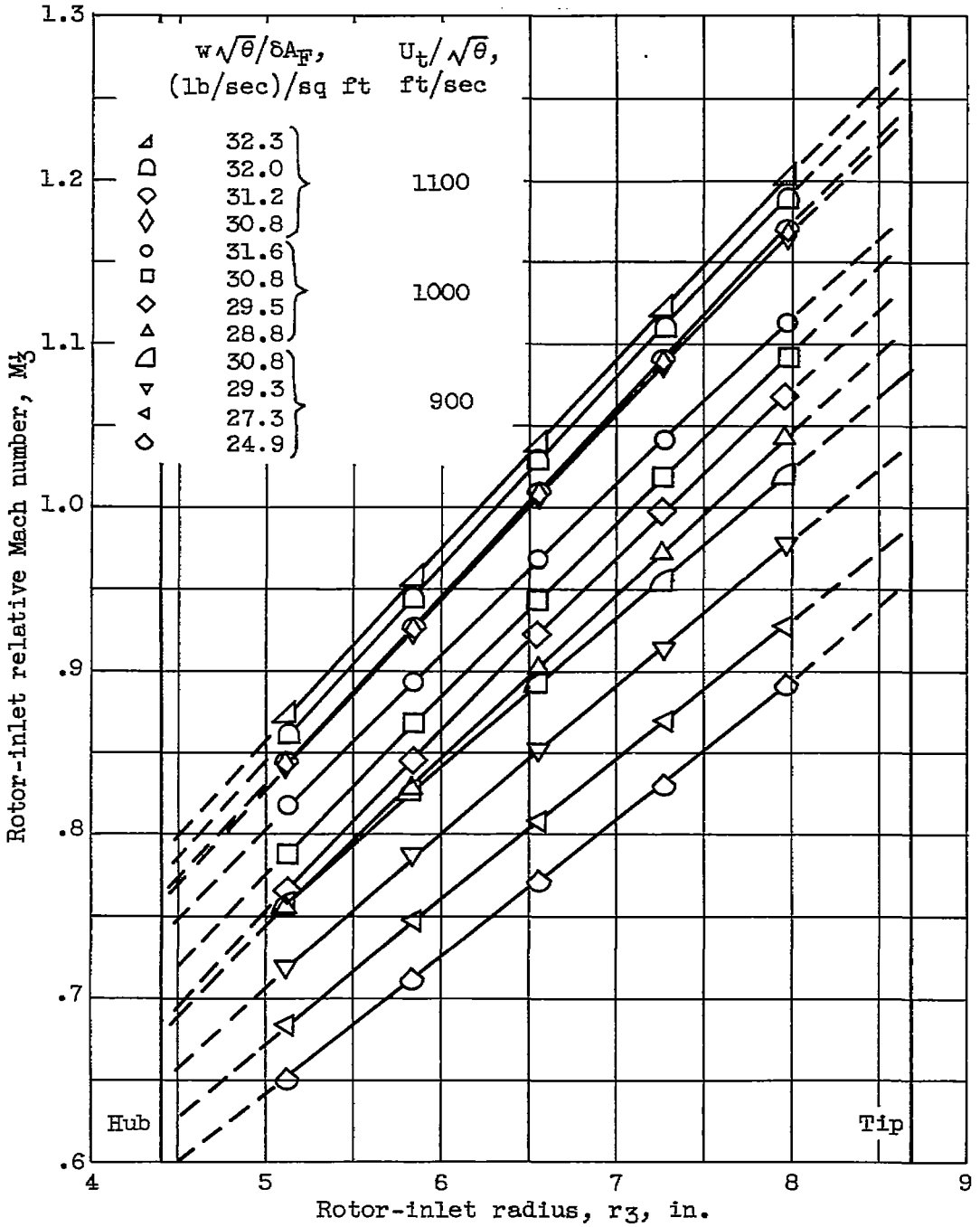

Figure 5. - Radial variation of rotor-inlet relative Mach number.

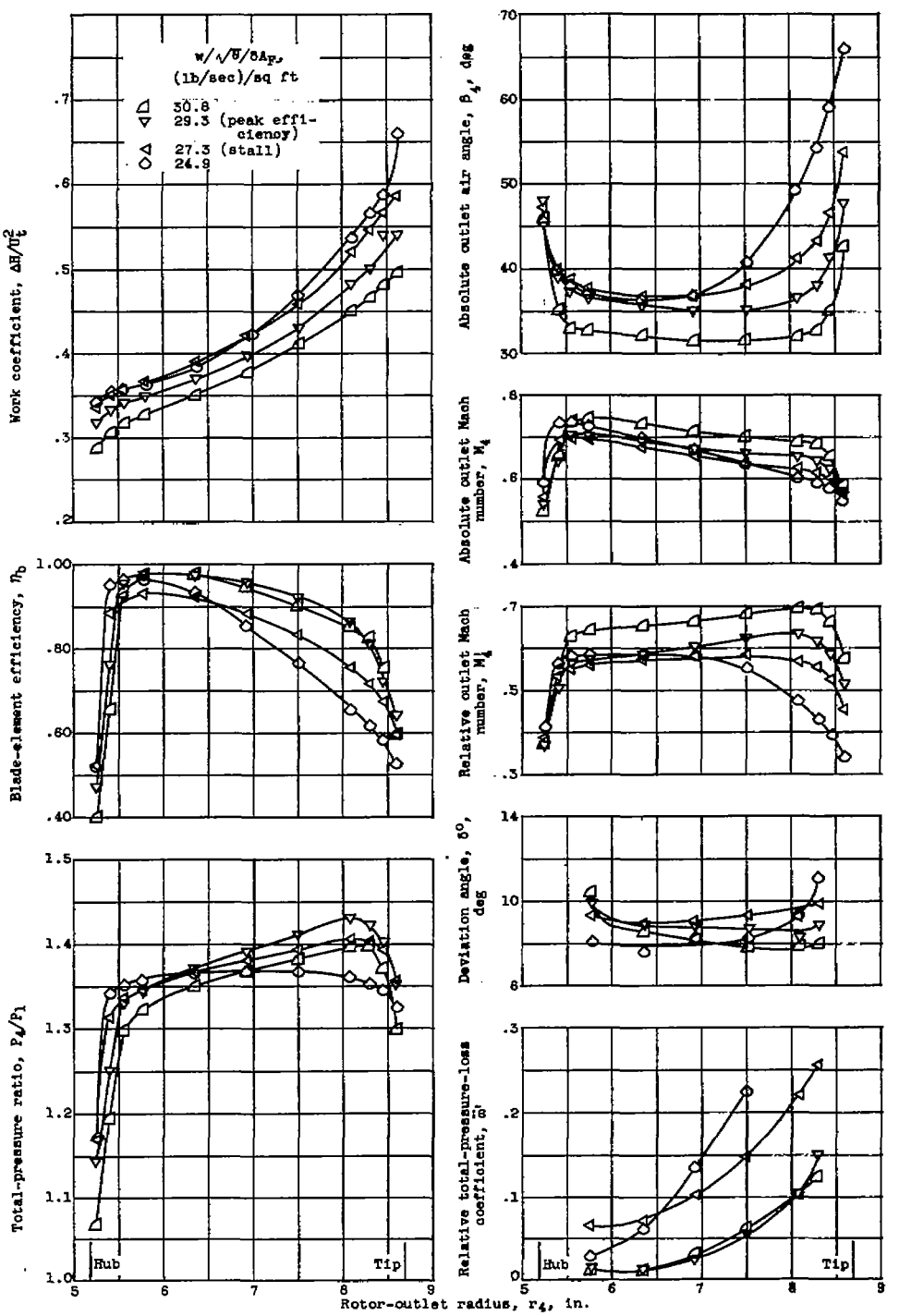

(a) Rotor corrected tip speed, 900 feet per second.

Figure 6. - Radial variations of blade-element characteristics and rotor-outlet conditions.

3888

3888

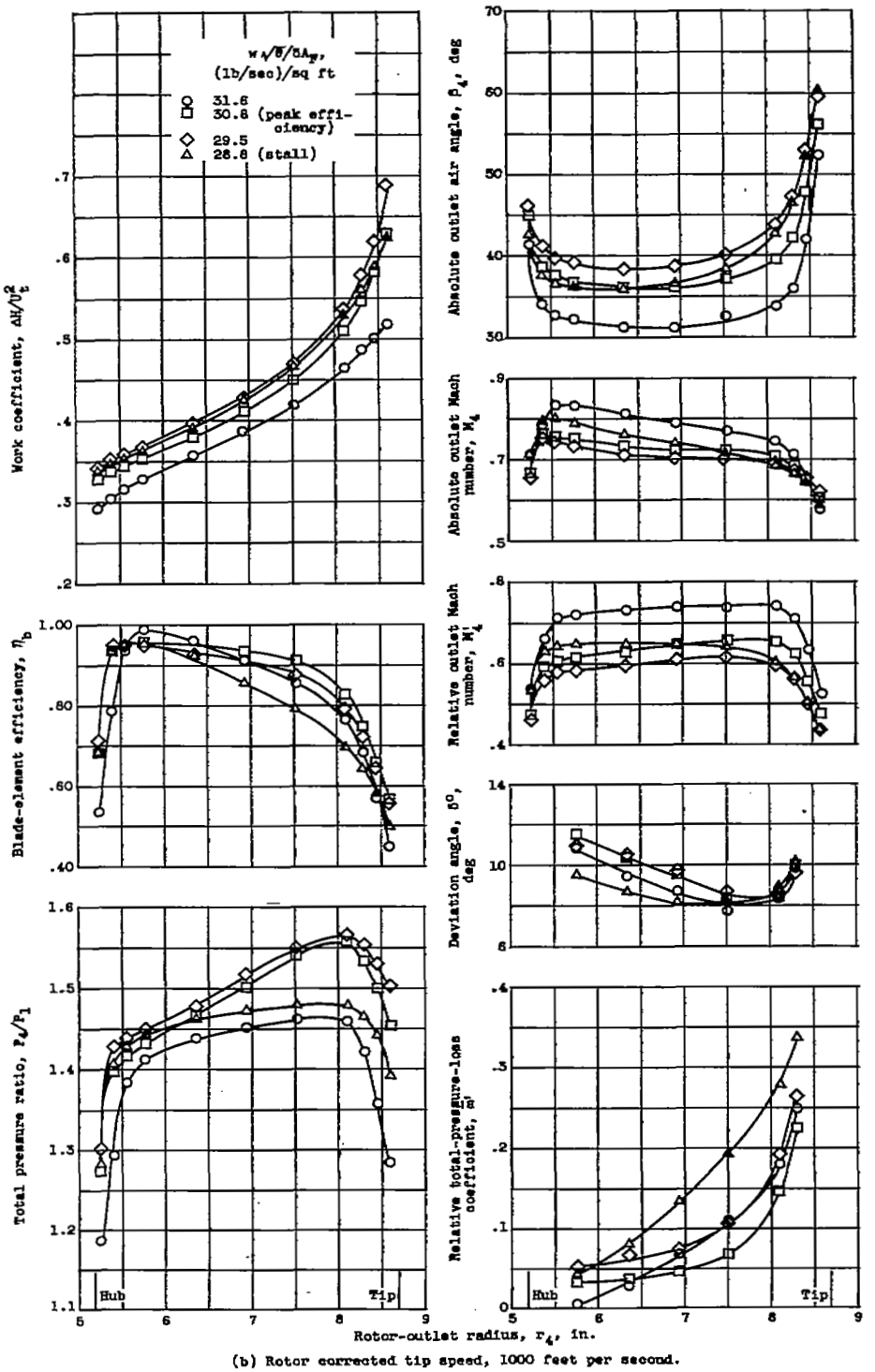

(b) Rotor corrected tip speed, 1000 feet per second.

Figure 6. - Continued. Radial variations of blade-element characteristics and rotor-outlet conditions.

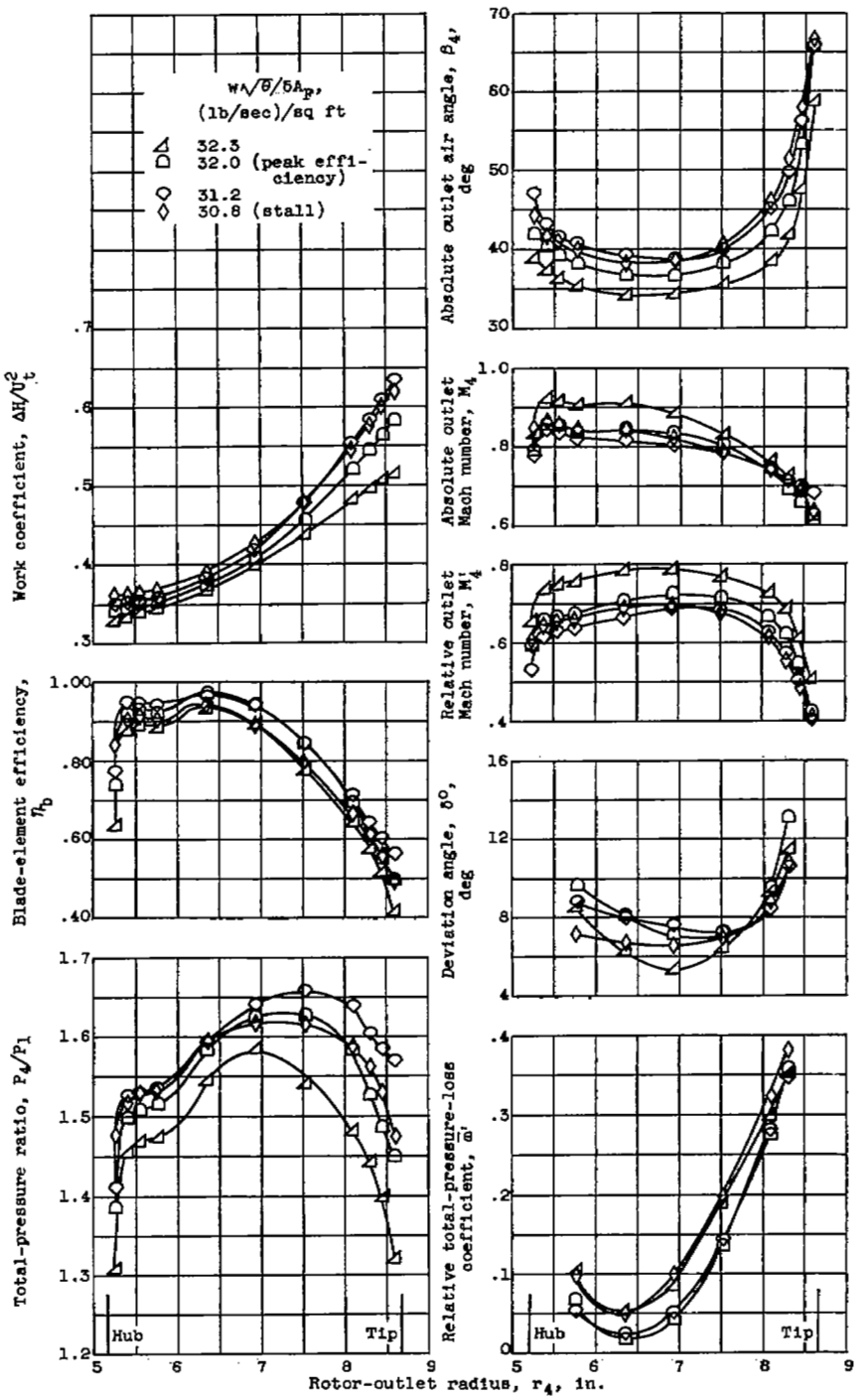

(c) Rotor corrected tip speed, 1100 feet per second.

Figure 6. - Concluded. Radial variations of blade-element characteristics and rotor-outlet conditions.

2888

3888 CN-5

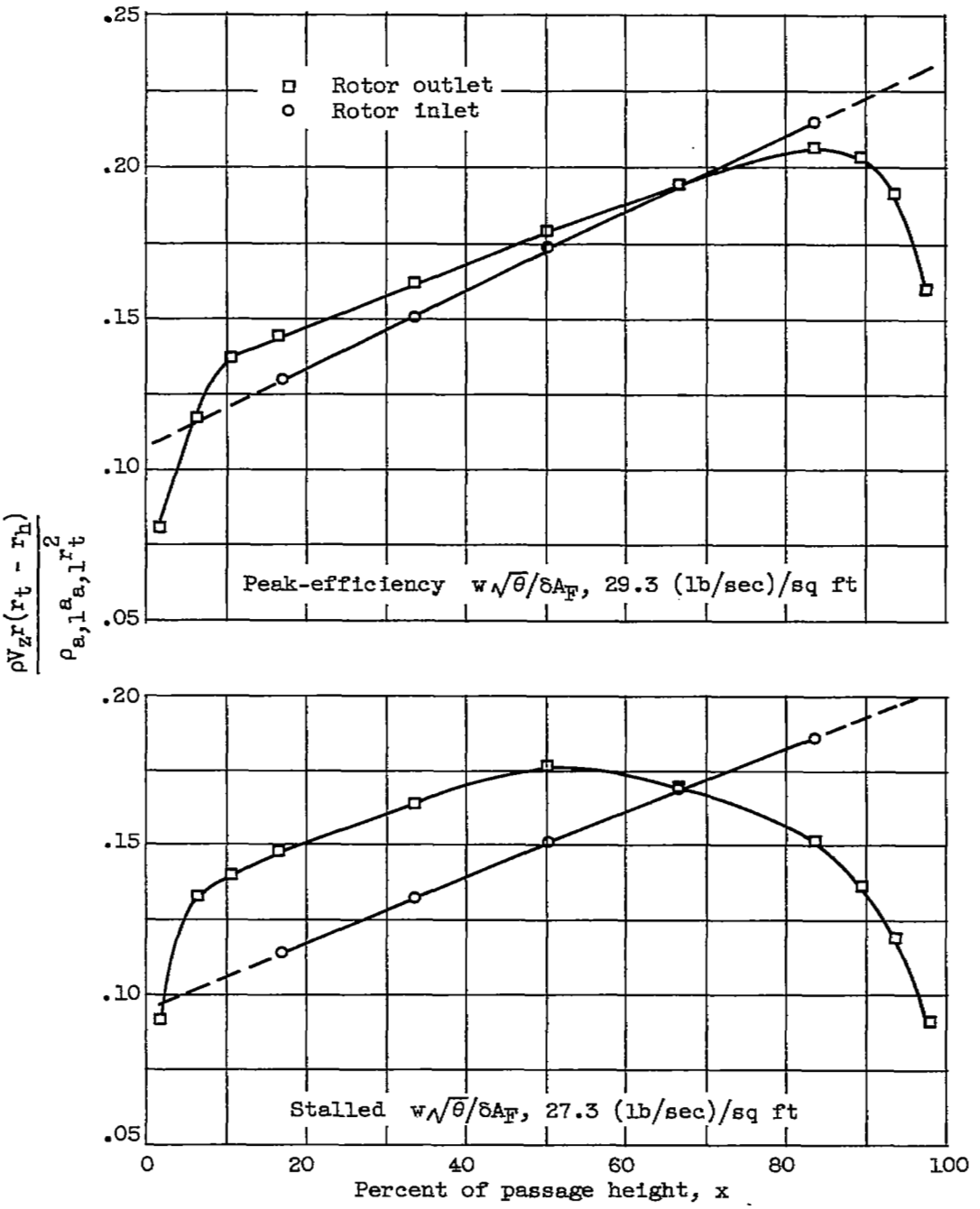

(a) Corrected tip speed, 900 feet per second.

Figure 7. - Radial distributions of weight flow at rotor inlet (station 2) and rotor outlet (station 4) for peak efficiency and stalled operation.

[redacted]

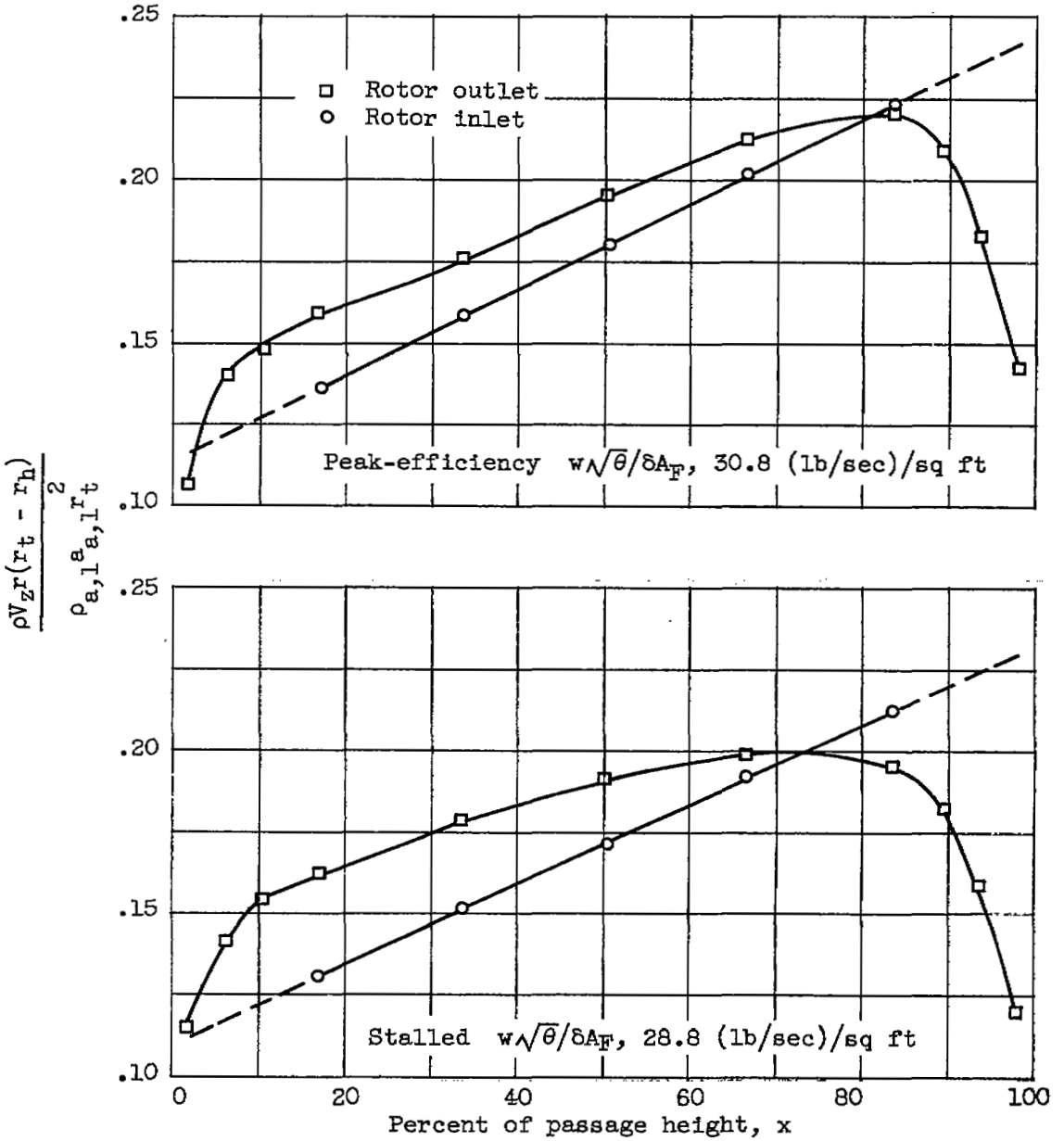

(b) Corrected tip speed, 1000 feet per second.

Figure 7. - Continued. Radial distributions of weight flow at rotor inlet (station 2) and rotor outlet (station 4) for peak efficiency and stalled operation.

3888

[redacted]

3888 CN-5 back

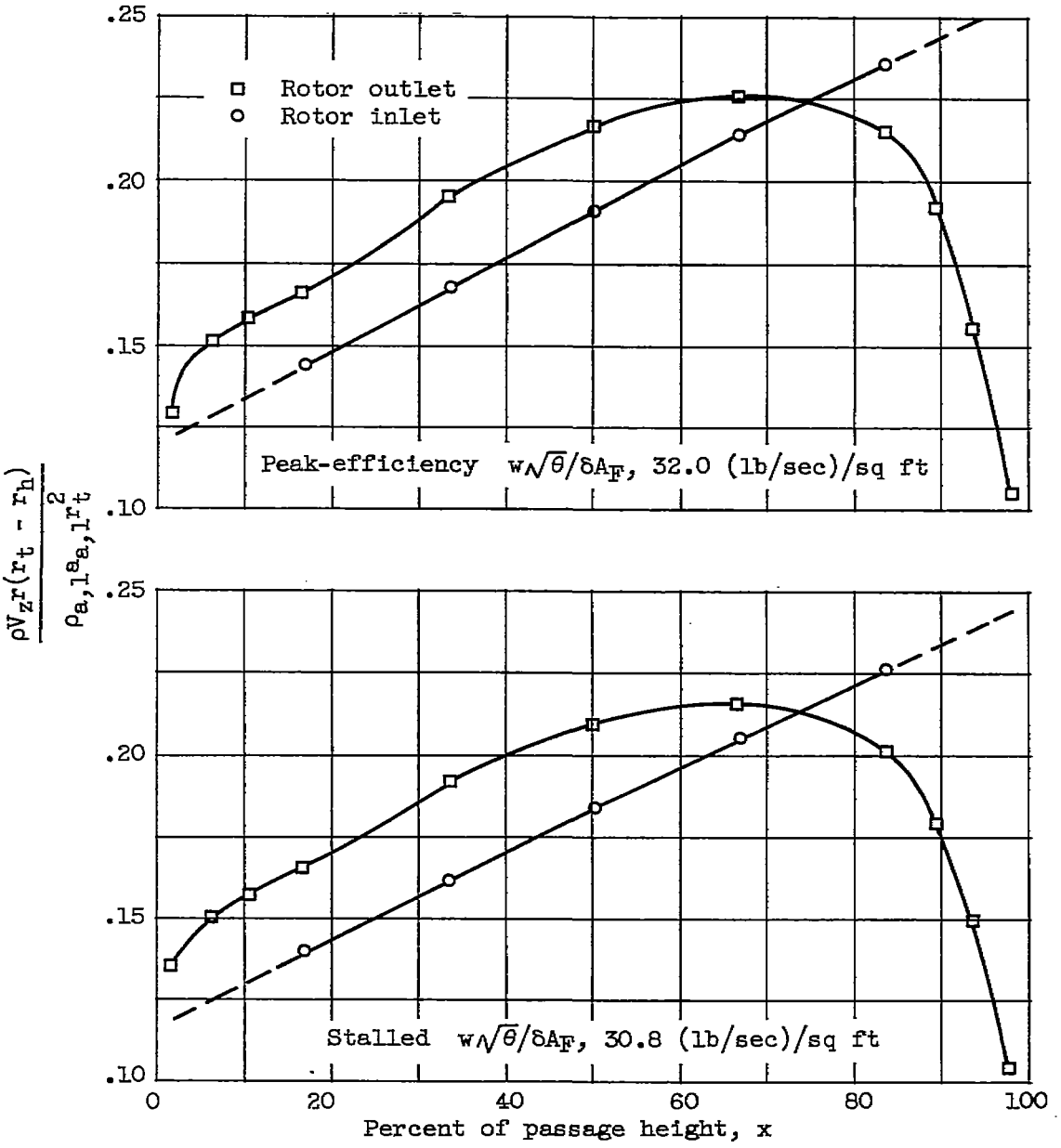

(c) Corrected tip speed, 1100 feet per second.

Figure 7. - Concluded. Radial distributions of weight flow at rotor inlet (station 2) and rotor outlet (station 4) for peak efficiency and stalled operation.

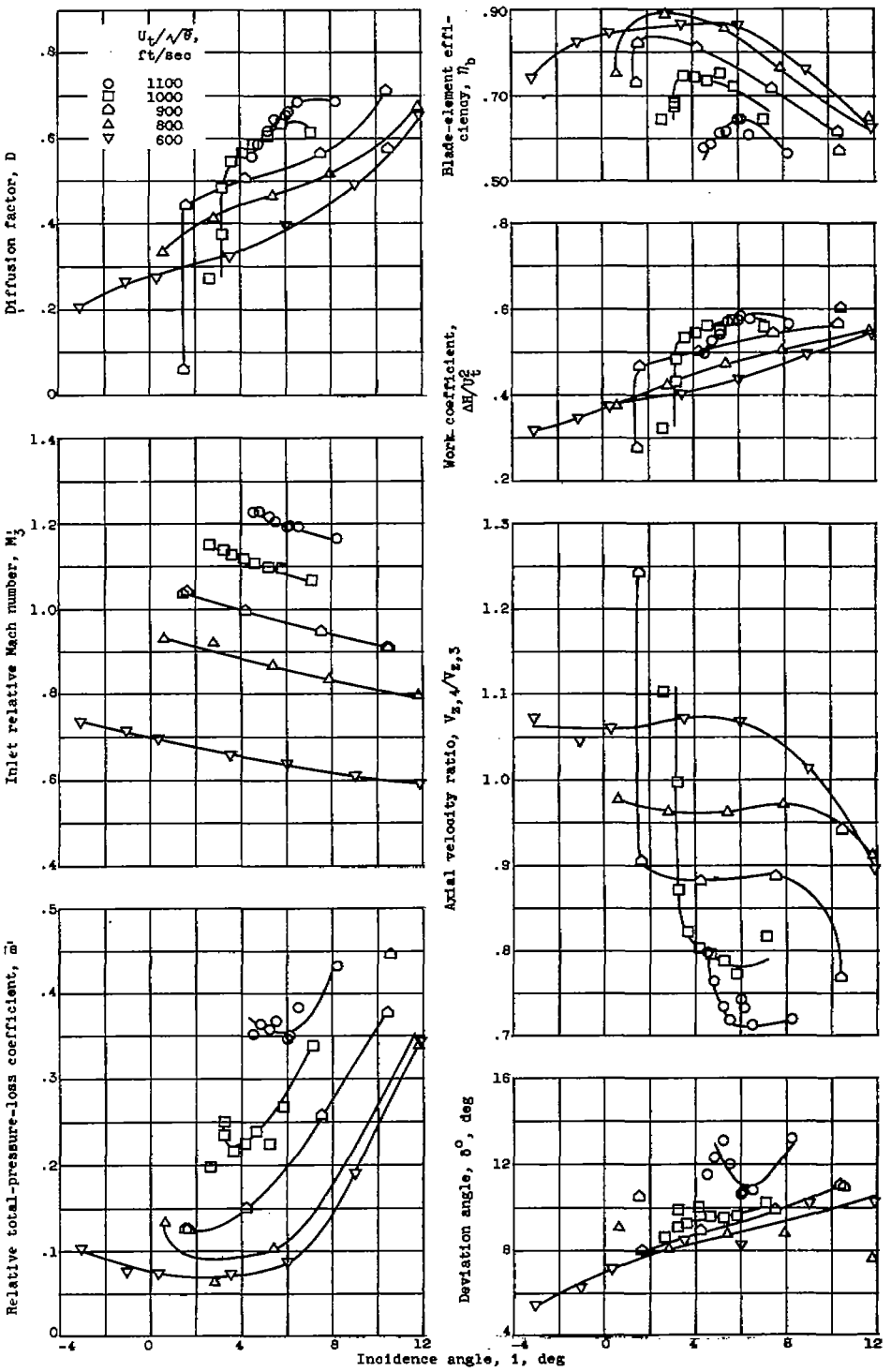

(a) Near tip; r_4 = 8.30 inches (11% from outer wall).

Figure 8. - Blade-element characteristics of low-blade-angle rotor.

3888

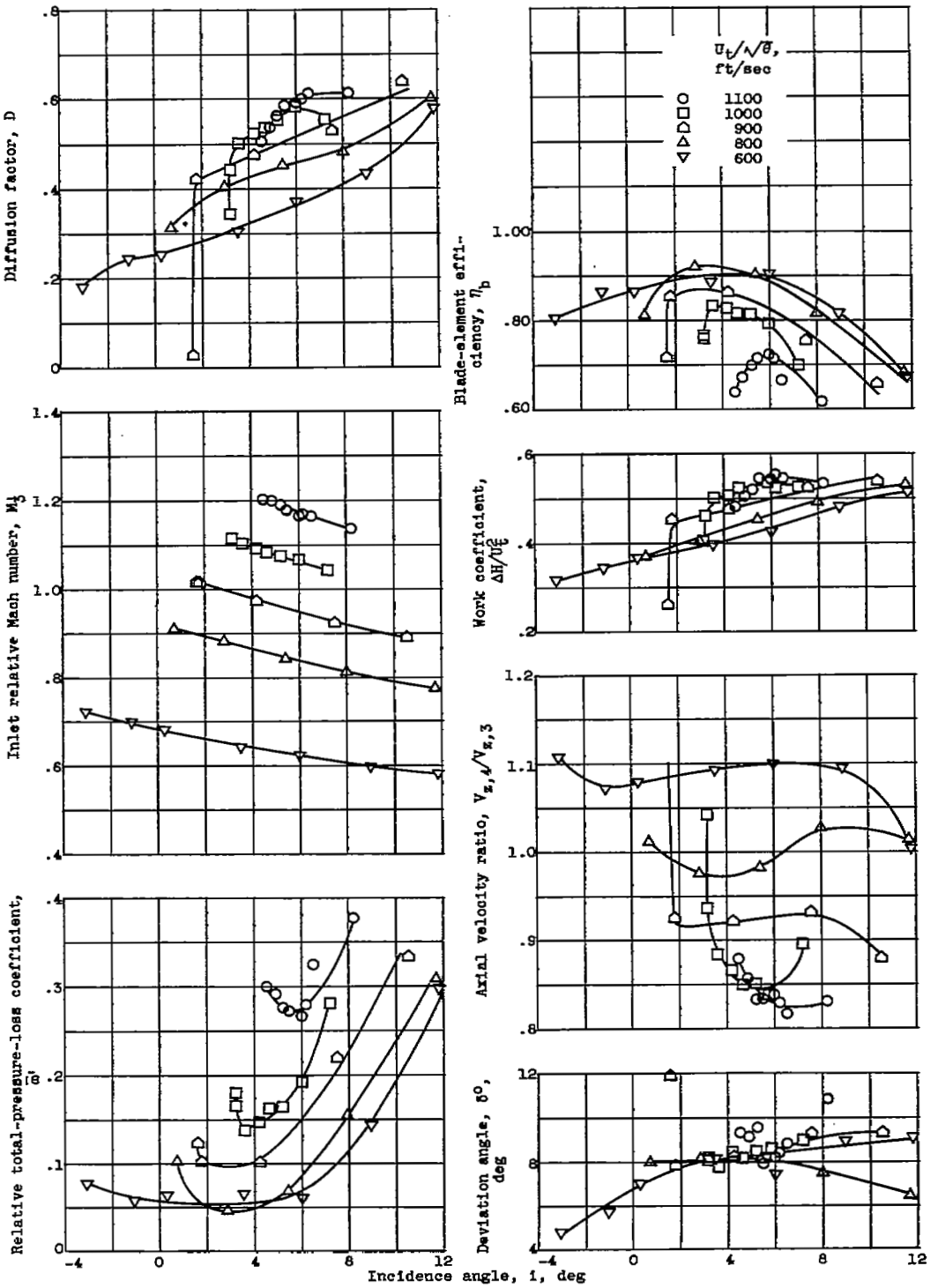

(b) Between tip and mean; r_4 = 8.10 inches (17% from outer wall).

Figure 8. - Continued. Blade-element characteristics of low-blade-angle rotor.

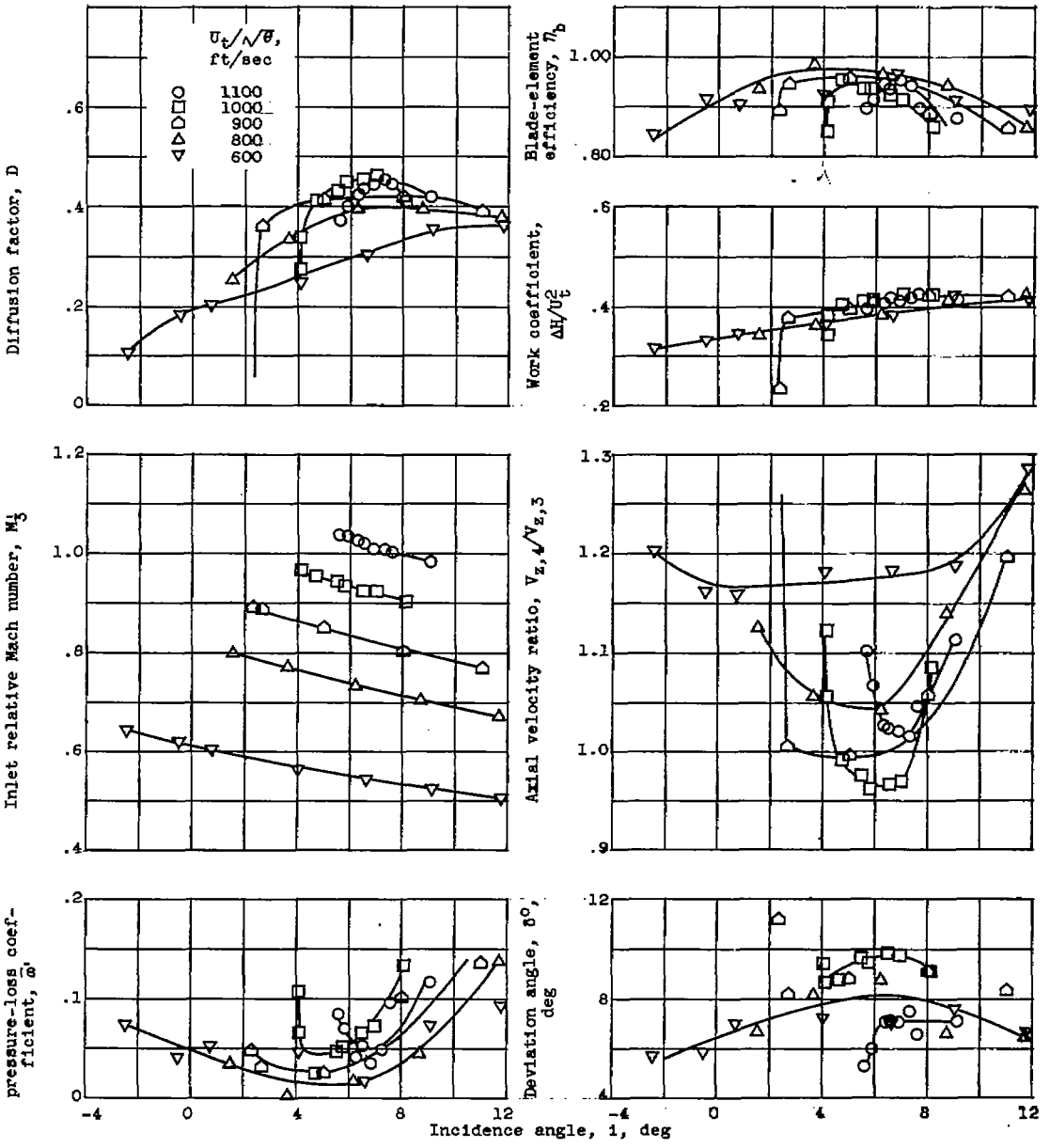

(c) Mean; r_4 = 6.93 inches.

Figure 8. - Continued. Blade-element characteristics of low-blade-angle rotor.

3888

3888

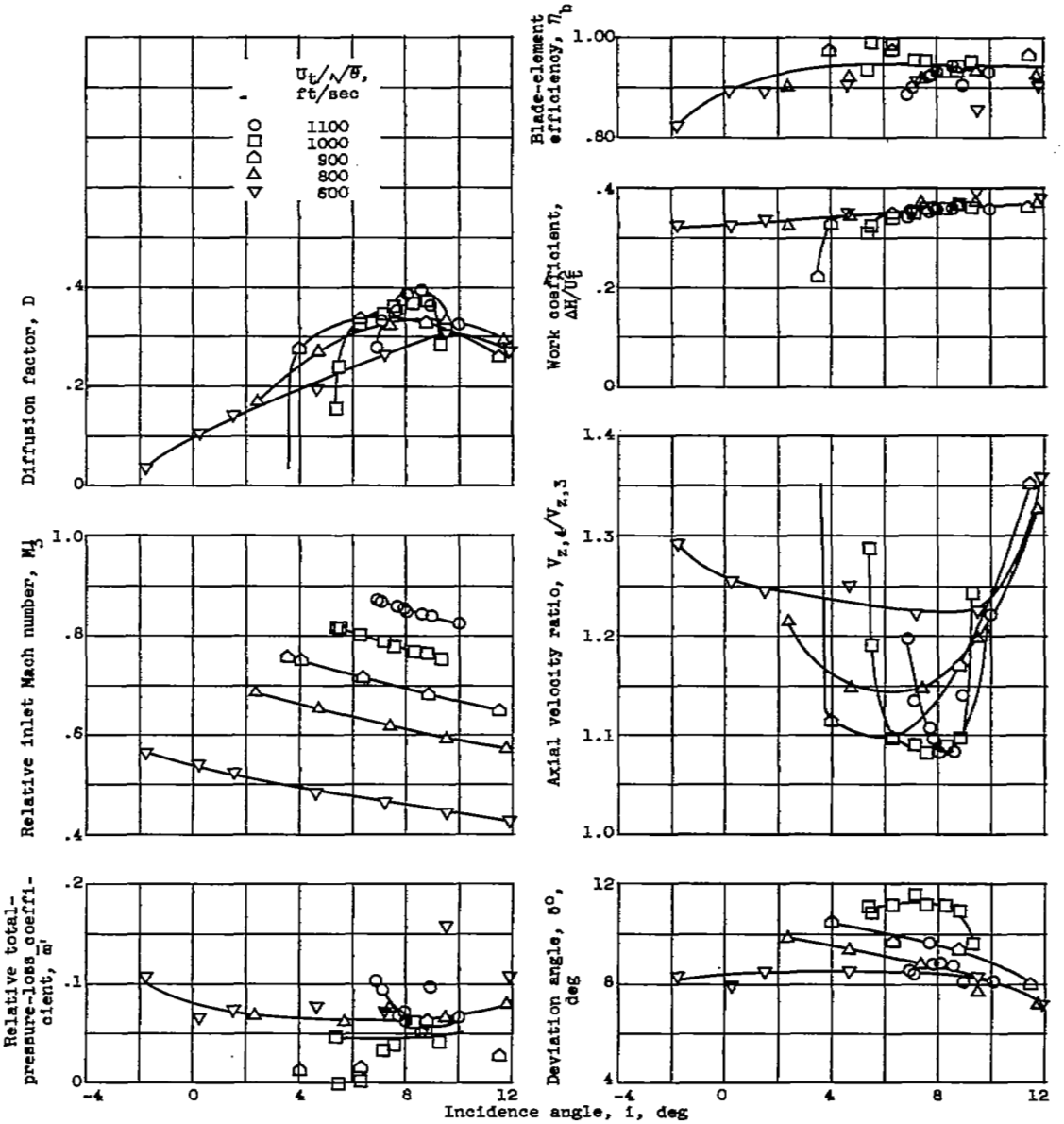

(d) Near hub; r_4 = 5.77 inches (83% from outer wall).

Figure 8. - Concluded. Blade-element characteristics of low-blade-angle rotor.

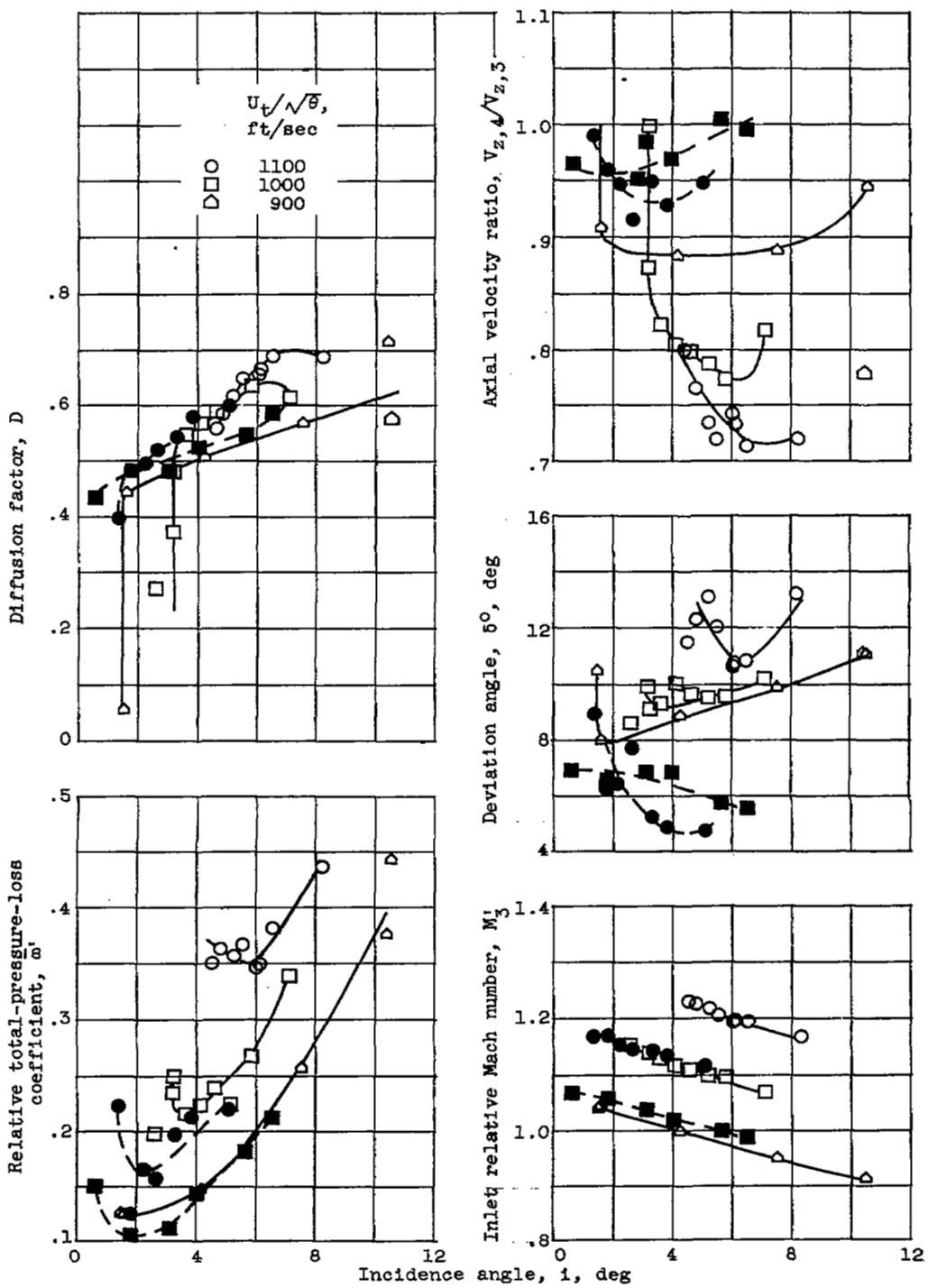

(a) Near tip; r_4 = 8.30 inches (11% from outer wall).

Figure 9. - Blade-element performance for original rotor (solid points) and low-blade-angle rotor (open points).

[redacted]

3888

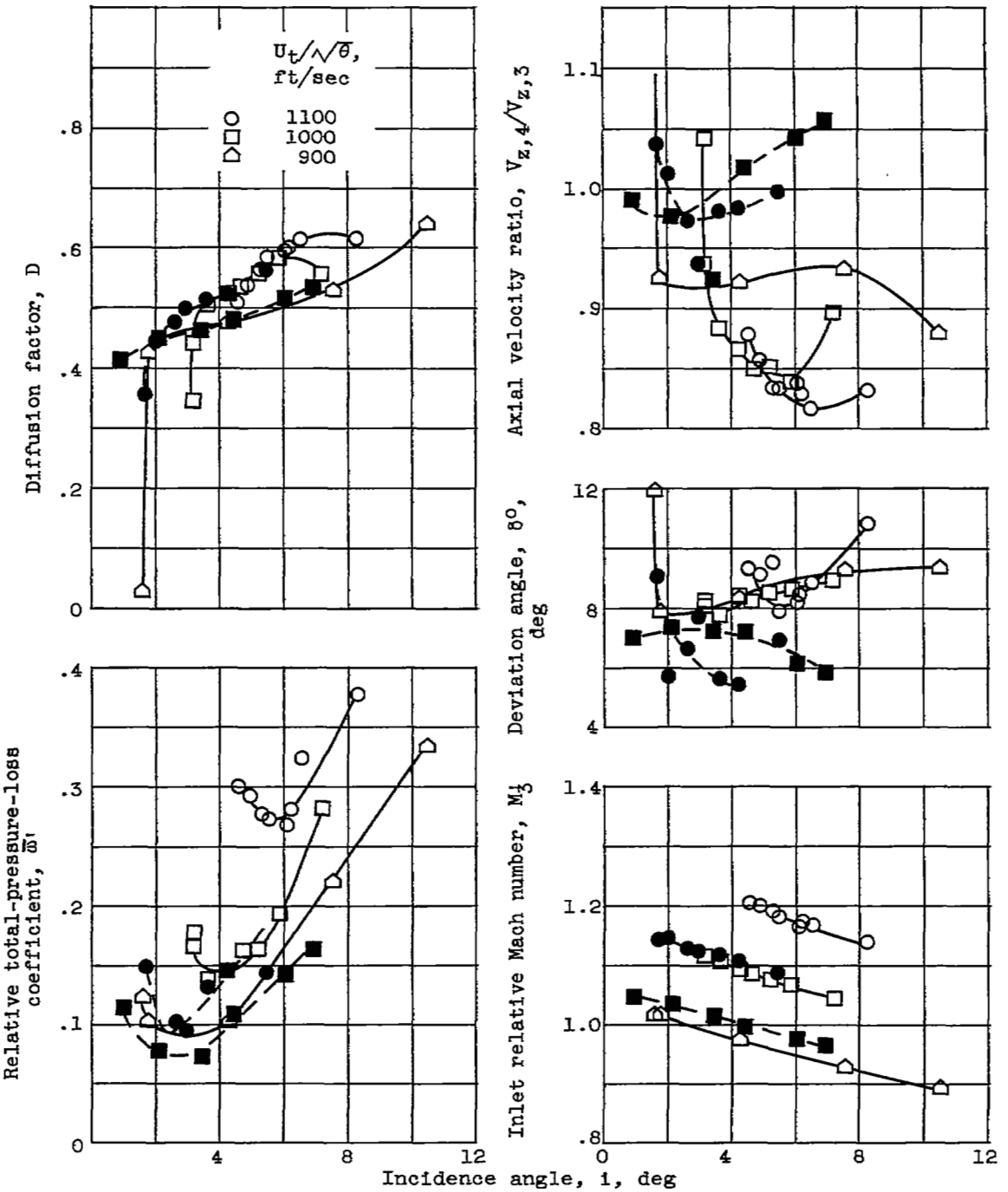

(b) Between tip and mean; r_4 = 8.10 inches (17% from outer wall).

Figure 9. - Continued. Blade-element performance for original rotor (solid points) and low-blade-angle rotor (open points).

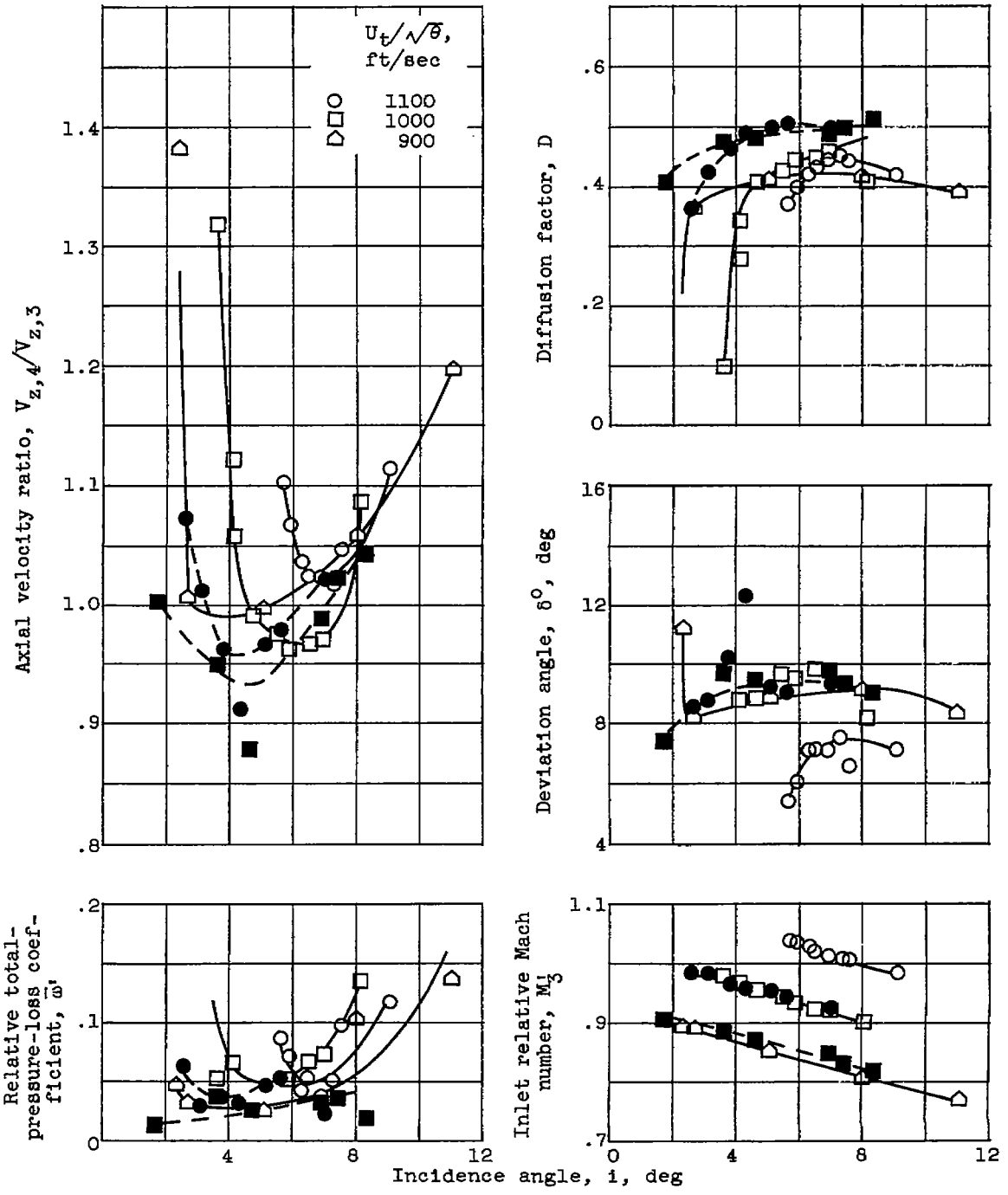

(c) Mean; r_4 = 6.93 inches.

Figure 9. - Continued. Blade-element performance for original rotor (solid points) and low-blade-angle rotor (open points).

[redacted]

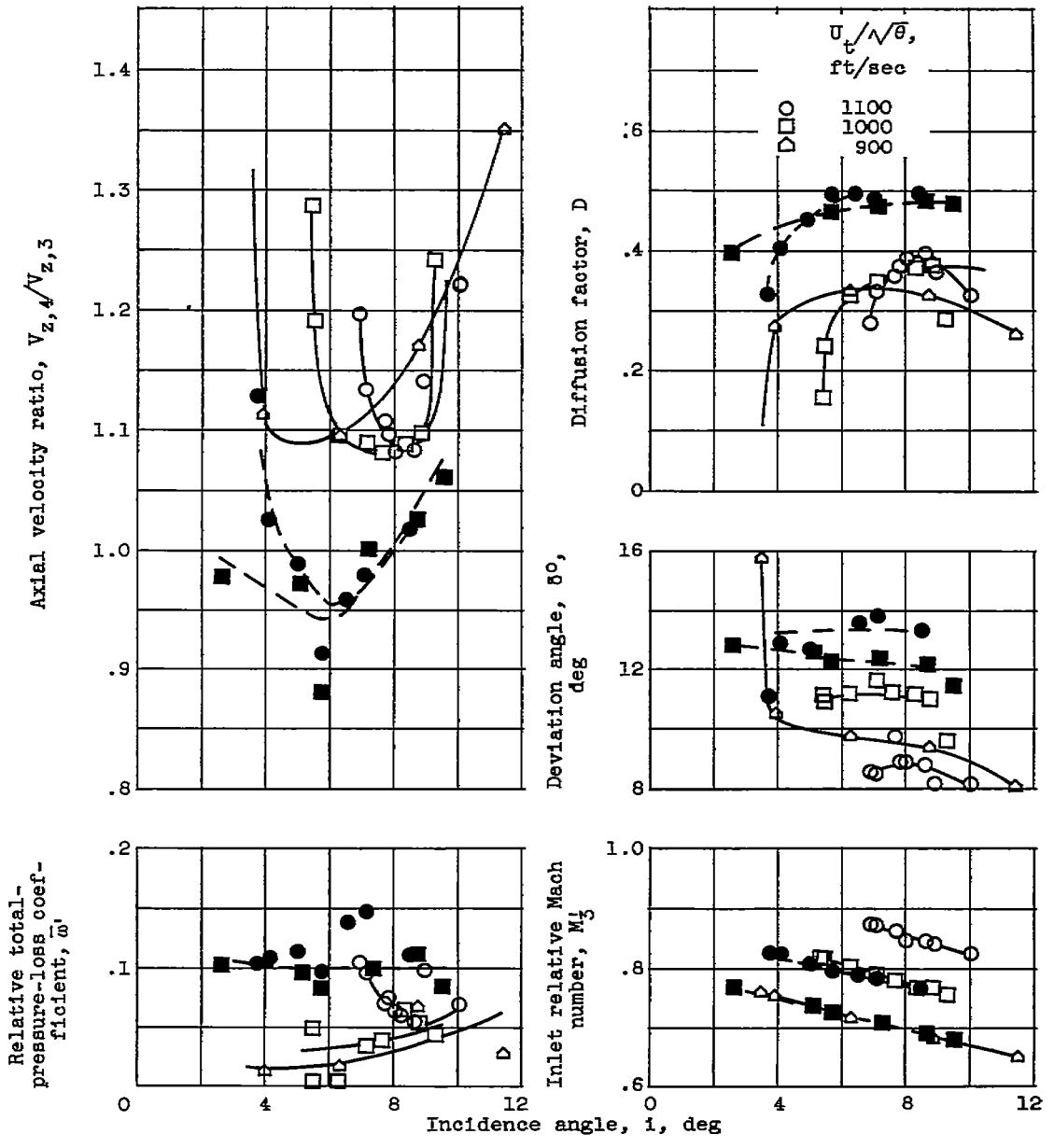

(d) Near hub; r_4 = 5.77 inches (83% from outer wall).

Figure 9. - Concluded. Blade-element performance for original rotor (solid points) and low-blade-angle rotor (open points).

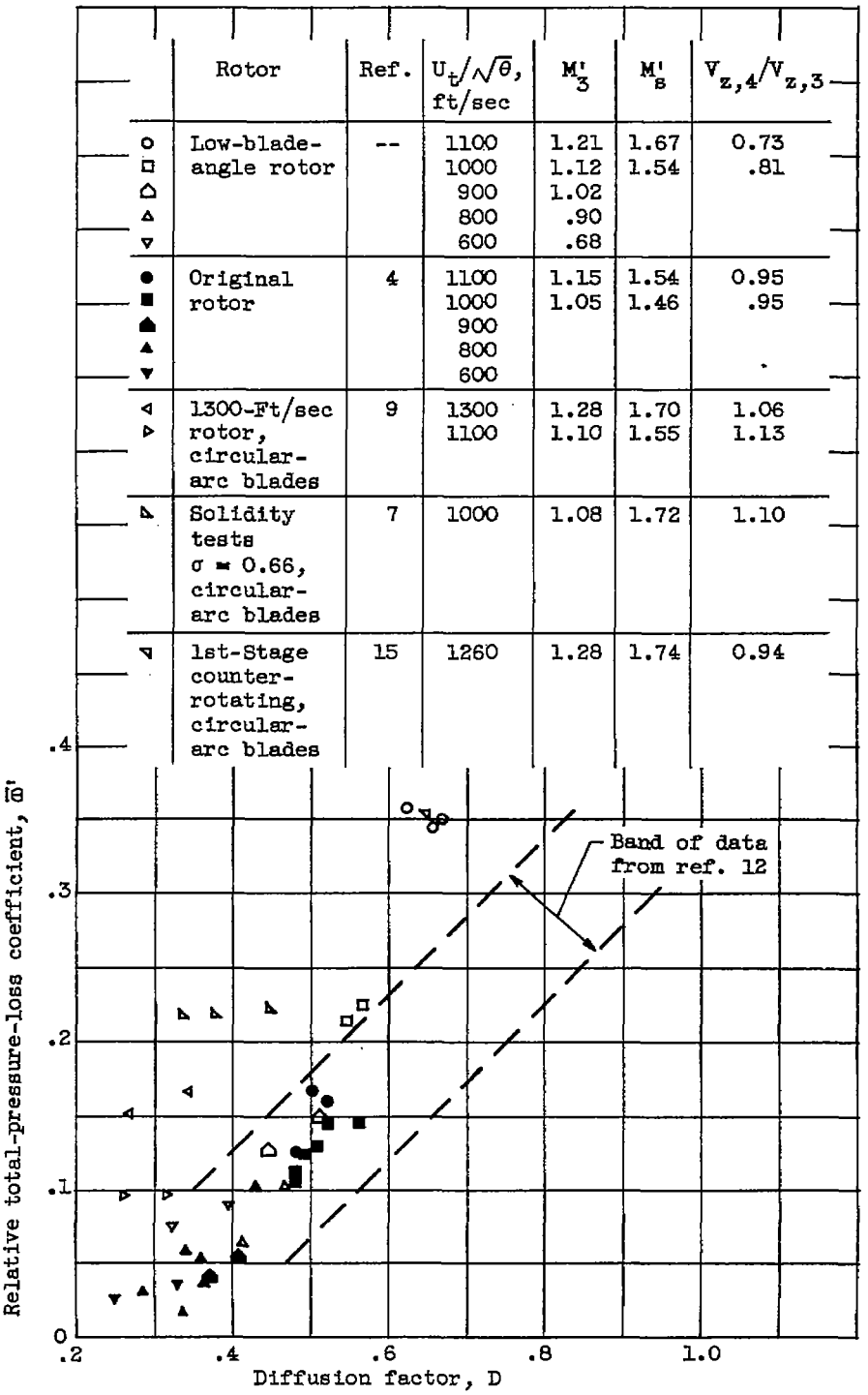

Figure 10. - Variations in tip-region relative total-pressure-loss coefficient with diffusion factor.

[redacted]

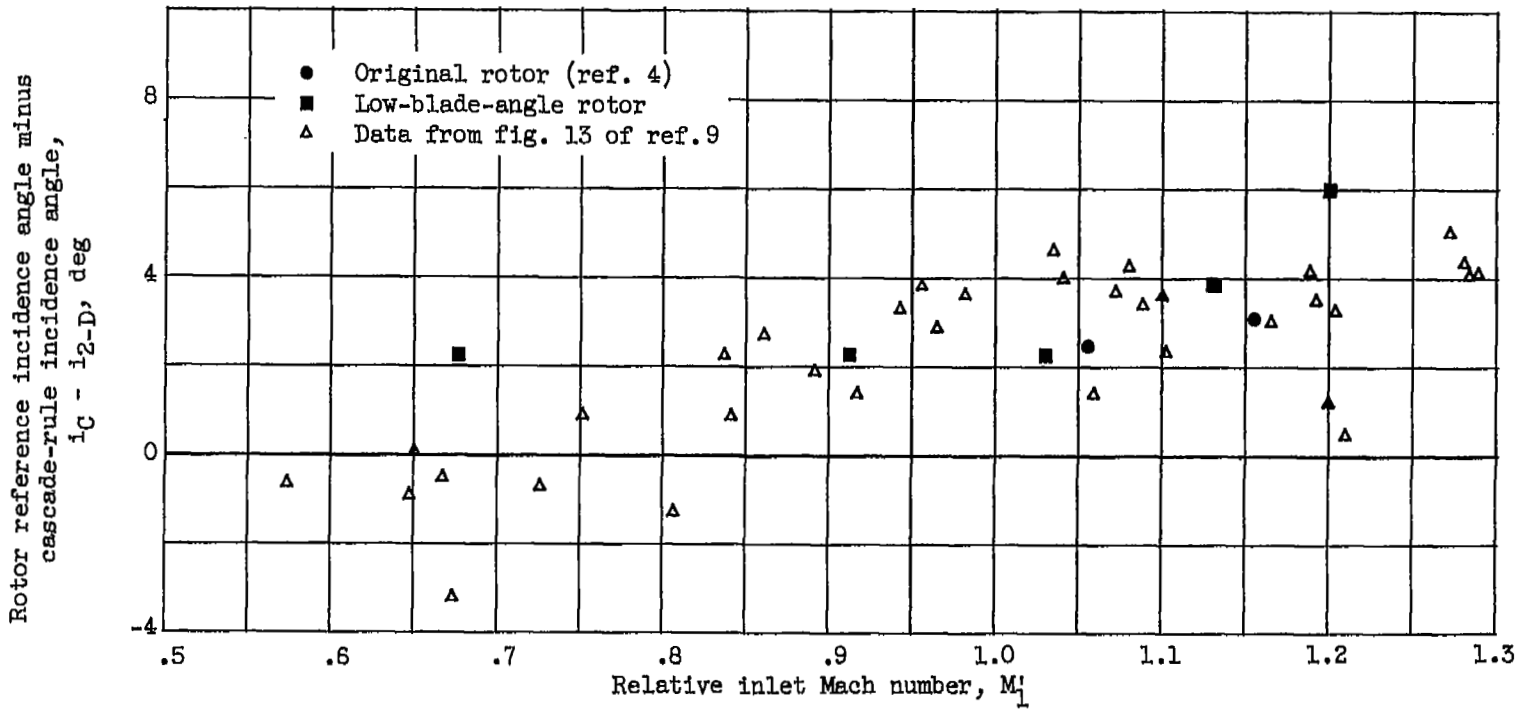

Figure 11. - Variation of rotor reference incidence angle minus two-dimensional-cascade-rule incidence angle with relative inlet Mach number for double-circular-arc blade sections near tip.

NACA - Langley Field, Va.

NASA Technical Library
3 1176 01436 0912